Phenylketonuria (PKU) is an inborn error of phenylalanine metabolism primarily treated through a phenylalanine-restrictive diet and frequently supplemented with an amino acid formula to maintain proper nutrition. PKU patients often report high levels of anxiety along with symptoms of gastrointestinal distress (i.e., chronic diarrhea, constipation, cramps); symptoms previously associated with gut microbiome dysbiosis. Little is known of the effects of these dietary interventions on the gut microbiome of PKU patients, particularly in adults.

The gut microbiome is a collection of microbes residing primarily in the large intestine. The colon is a major production site for short chain fatty acids (SCFAs) through anaerobic fermentation by commensal bacteria. SCFAs provide a source of energy for the colonocytes, as well as provide anti-inflammatory benefits. The production of SCFA appears to be dependent on the availability of soluble fibers and members of the gut microbiota capable of fermentation.

We characterized the gut microbiome of adults with PKU for the first time and identified signs of dysbiosis. We then focused on the synthetic, low fiber, nature of the amino acid diet in a murine model. In this interdisciplinary study, we monitored the effect of a consuming synthetic diet on the composition of the murine gut microbiome over the course of 13 weeks, beginning at weaning. At the conclusion of the feeding period, mice we observed for anxiolytic behavior, locomotion, and cognition. We also searched for markers of inflammation through colon shrinkage, changes in cytokine levels within several tissues, and determined the concentration of SCFAs in the colon at the conclusion of the feeding period.

The gut microbiome of mice fed the synthetic diet experienced significant deviation from the control group which affected relative abundance of beneficial bacteria. Mice on the synthetic diet were found to have shorter colons, lower concentration of SCFAs in the colon, and demonstrated elevated exploratory behavior.

Effects of a Synthetic Amino Acid Diet: Insights

from the Gut Microbiome, Inflammation, and Behavior

Viviana J Mancilla, BS

APPROVED:

_____

Major Professor

_____

Committee Member

_____

Committee Member

_____

Committee Member

_____

University Member

_____

Chair, Department of Microbiology, Immunology, and Genetics

_____

Dean, Graduate School of Biomedical Sciences

THE UNIVERSITY *of* NORTH TEXAS
HEALTH SCIENCE CENTER *at* FORT WORTH

EFFECTS OF A SYNTHETIC AMINO ACID DIET: INSIGHTS FROM THE GUT MICROBIOME, INFLAMMATION, AND BEHAVIOR

DISSERTATION

Presented to the Graduate Council of the
Graduate School of Biomedical Sciences

University of North Texas
Health Science Center at Fort Worth
in Partial Fulfillment of the Requirements

For the Degree of

DOCTOR OF PHILOSOPHY
BIOMEDICAL SCIENCES

By

Viviana J Mancilla, BS
Fort Worth, Texas
April 2021

ACKNOWLEDGMENTS

I would like to thank my major professor, Dr. Michael S. Allen for his mentorship in the development of my research questions. Your insightful feedback pushed me to think more critically and brought my work to a higher level. Thank you to my former and current lab members for being patient with me while I learned as well as providing me with an outlet to give back and teach.

I would also like to acknowledge my committee: Dr. Harlan Jones, Dr. Nicole Phillips, Dr. John Planz, and Dr. Dorette Ellis. Thank you for your questions and for preparing me over the past five years. Dr. Xavier Gonzales, thank you for believing in me and pushing me to apply to graduate school. You really saw potential in me and never let me forget it.

I was lucky to have made several friends throughout my time at UNTHSC. I want to specifically highlight Carmen for being a constant voice of reason and someone I could always count on. Thank you to Courtney, Danielle, Gita, and Talisa for making our office space simultaneously the most collaborative and disruptive place on campus.

Thank you to my family and partner for their patience, love, and support. Thank you for never having any reservations toward me following my own path. To my parents, I acknowledge the sacrifices that have been made for me to get to where I am, and I owe this all to you.

Finally, I would like to thank Max and Oliver for keeping me sane and active throughout even the most stressful points.

TABLE OF CONTENTS

LIST OF TABLES

LIST OF ILLUSTRATIONS

Figure 2. Pairwise comparison (DESeq2 analysis). Differentially abundant ASVs ($p < 0.001$) in PKU patients and non-PKU control counterpart samples are shown. ASVs were assigned to the genus (y-axis) and phylum level (colors). Negative "log2 Fold Change" values (x-axis) indicate higher abundance in PKU samples and positive values indicate higher abundances in control samples.

Figure 3. Phylofactorization of all bacterial ASVs present in PKU and control fecal samples (**A**). Three factors were identified as the most influential members differentiating PKU and control samples at the genus level: (**B**) *Romboustia* (green), (**C**) two unknown *Lachnospiraceae* (purple), and (**D**) *Enterocloster* (orange).

Figure 4. Alpha diversity for PKU and control samples. Statistical significance of the (A) number of observed ASVs and (B) Shannon diversity index from PKU and control samples were calculated and compared with the Wilcoxon rank-sum test. Median scores are represented with a horizontal line, the box outer limits represent the first to third quartiles, the whiskers indicate the range of measurements for each group, and each point denotes a sample. Observed ASVs (Wilcoxon: W = 143, $p = 0.28$) and Shannon index (Wilcoxon: W = 139, $p = 0.37$).

Figure 5. Genus-level beta diversity comparison of the gut microbiota compositions. based on principal component analysis (PCA) of PhILR distances for PKU (orange) and control (green) samples. Each point represents a sample, and the condition is denoted by its color; larger circles represent the mean coordinates for each group.

Figure 6. The relative abundance of predicted microbial genes related to metabolism in control (blue) and PKU (orange) samples was based on Welch's t-test ($p \leq 0.05$). The colored bars represent 95% confidence intervals calculated using Welch's inverted method. The colored circles represent the difference in mean proportions between PKU and control samples.

Chapter III: A synthetic formula amino acid diet leads to microbiome dysbiosis, reduced colon length, and secondary markers of inflammation in a murine model

Figure 1. Diagram of experimental design to investigate the effects of consuming a synthetic formula diet on behavior, gut microbiome, and inflammation. Tissue types are denoted by illustrations described in the legend and represented by a letter beneath the assay in which they were examined (A – Stool; B – Colon; C – Blood (serum); D – Hippocampus).

Figure 2. Divergence of gut microbiota alpha diversity (left: number of observed ASVs; right: Shannon diversity index) based on assigned diet plotted from week 0 (weaning) through week 13.

Figure 3. Principal component analysis (PCA) of PhILR distances for the gut microbiota of synthetic and standard diet animals after 13 weeks of feeding on the assigned diet. Individual samples are represented by one point; larger circles represent the mean coordinates for each diet group. (R2 = 0.56, $p = 0.001$)

Figure 4. DESeq2 analysis of stool samples collected at week 13 of the feeding period found 76 differentially abundant bacterial genera (y-axis) with in eight phyla (denoted by color). Negative "log2 Fold Change" values (x-axis) indicate higher abundance in synthetic diet animal samples and positive values indicate higher abundances in standard diet animal samples.

Figure 5. Phylofactorization of all bacterial ASVs present in stool samples from mice fed either a synthetic or standard diet at week 13 (**A**). Three factors (family clades) were identified as drivers of variation between the two diet groups: (**B**) *Erysipelotrichaceae* (purple), (**C**) *Prevotellaceae* (blue), and (**D**) *Muribaculaceae* (yellow). ($***p \leq 0.001$)

Figure 6. PICRUSt2 analysis predicted 14 metabolic pathways may be affected by the consumption of the synthetic formula diet (coral) compared to the standard diet (blue), based on microbiota present in the gut microbiome in mice in each dietary group at week 13. The colored bars represent 95% confidence intervals calculated using Welch's inverted method ($p \leq 0.05$ with Bonferroni corrections for multiple comparisons. The colored circles represent the difference in mean proportions between synthetic diet and standard diet animal samples.

Figure 7. Mouse body weights and colon length measurements of mice fed the synthetic diet or the standard diet after 13 weeks. Body weight for all mice was measured weekly throughout the 13-week feeding period (**A**). Synthetic diet animals (7.85 cm ± 0.65) had a significantly shorter colon than that of standard diet animals (9.83 cm ± 0.48), $p = 2.65 \times 10^{-07}$ (**B**). Representative photos of colons dissected from synthetic diet animals (**C** – left) and standard diet animals (**C** – right). ($***p \leq 0.001$)

Figure 8. SCFA concentrations (mmol/kg) in colon tissue of mice fed the synthetic diet or the standard diet after 13 weeks. (**A**) Acetic acid synthetic mean (7.43 ± 3.17), standard mean (16.39 ± 8.58), t-test one tail $p = 0.04$; (**B**) Propionic acid synthetic mean (2.31 ± 0.96), standard mean

(4.34 ± 2.02), t-test one tail $p = 0.04$; (**C**) Butyric acid synthetic mean (1.09 ± 0.56), standard mean (4.16 ± 2.04), t-test one tail $p = 0.01$. (*$p \leq 0.05$; **$p \leq 0.01$)

Figure 9. Cytokine (TNF-α, IL-6, IL-10) quantification in the serum, hippocampus tissue lysate (brain), and colon tissue lysate (gut). (**A**) Serum TNF-α*; (**B**) Serum IL-6*; (**C**) Serum IL-10; (**D**) Hippocampal TNF-α*; (**E**) Hippocampal IL-6***; (**F**) Gut TNF-α; (**G**) Gut IL-6; (**H**) Gut IL-10**. Hippocampal IL-10 was excluded. *$p \leq 0.05$; **$p \leq 0.01$; ***$p \leq 0.001$

Figure 10. Open Field Test. An independent samples *t*-test was used to compare behavior in the open field chamber between animals fed synthetic diet (coral) and a standard diet (blue) for (**A**) total time spent in the center zone, (**B**) total distance traveled, (**C**) total average speed, and (**D**) total vertical counts. While all cases revealed higher average values for synthetic diet fed mice, only total average speed (C) was significantly different (*$p \leq 0.05$).

Figure 11. Elevated Zero Maze. (**A**) Total distance traveled in synthetic and standard diet animals; (**B**) Total time in open areas; (**C**) Number of entries into the open areas or zones; (**D**) Latency to first entry into an open zone; (**E**) Total average speed. No significant differences were detected by independent samples *t*-tests.

Figure 12. Contextual Fear Conditioning. An independent samples *t*-test revealed no significant difference in percent freezing time between synthetic and standard diet animal following a footshock training day ($t(18) = -0.26$, $p = 0.80$, $n = 10$).

CHAPTER I

INTRODUCTION

Background

Phenylketonuria

Phenylketonuria (PKU) is an autosomal recessive disease, caused by mutations in both alleles of the *PAH* gene and affects approximately 1:10,000 births per year. The result is an enzyme deficiency that prevents the metabolism of phenylalanine, an essential amino acid, to tyrosine via the enzyme phenylalanine hydroxylase (PAH, **Figure 1**). Without the functional enzyme, accumulation of phenylalanine (Phe) and its partial metabolic intermediates, as well as a lack of tyrosine, can lead to mental retardation, behavioral, neurologic and metabolic issues [1].

Currently, the primary treatment for PKU patients is restriction of dietary Phe and supplementation via a synthetically formulated amino acid diet [2]. The bulk of the diet includes formula made of single amino acids, not including phenylalanine, and allows for the consumption of most fruits and vegetables in limited quantities. Compliance to the diet is an issue among patients and can lead to nutritional deficiencies, gastrointestinal upsets, and behavioral issues [3].

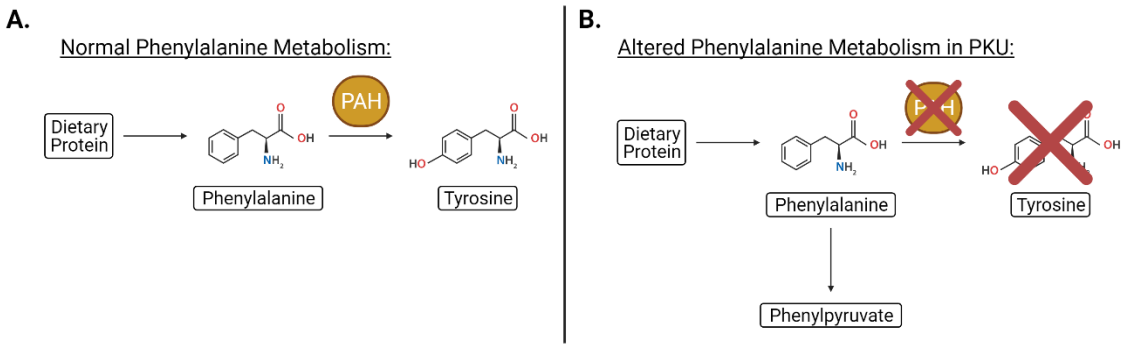

Figure 1. Phenylalanine metabolism in healthy and PKU system. (**A**) The metabolic pathway of phenylalanine to tyrosine vs (**B**) the alternative metabolic pathway of phenylalanine to phenylpyruvate due to the disfunction of phenylalanine hydroxylase in PKU patients. This alternative pathway leads to increased concentration of Phe and Phe derivatives in the blood.

The Microbiome

The gut microbiome is a dynamic collection of about 100 trillion microbes that reside within the gut that can be modulated by the host in the form of dietary intake, antibiotic use, and host genetics [4-9]. Although the microbiome also includes the genetic content of fungi, viruses, and archaea, it is dominated by bacteria, which serve as the focus for these studies. The microbiome can in part educate the immune system, act as a metabolic organ, degrade toxins from food, prevent pathogen invasion, and produce certain vitamins and amino acids for absorption by the host [10]. Germ-free mice (born via caesarean section, raised in sterile environments) lack a residential microbiome and have shown light on the impact of the microbiome on the host; they also have decreased immune function, behavioral disorders, and nutritional deficiencies [11, 12]. A healthy microbiota balance is essential for host health and wellbeing, while dysbiosis in the gut has been linked to inflammation and disease [13, 14].

Fermentation

The colon provides an environment for anaerobic fermentation of ‘indigestible food products’, also referred to as fiber or microbiota-accessible carbohydrates (MACs). Fermentation

of fibers that are indigestible by the human system produces short chain fatty acids such as acetate, propionate, and butyrate via substrate-level phosphorylation as a result [15]. Short chain fatty acids (SCFAs) have been shown to be protective against colitis and general inflammation in the gut by decreasing the colonic pH, neutralizing toxins, and preventing the adhesion of pathogenic microbes in the gut (**Figure 2**) [16-20]. Additionally, SCFAs beneficially modulate the immune system by downregulating chronic inflammation without impeding the inflammatory response to pathogen invasion [21, 22]. Butyrate in particular has been shown to be the main energy source for colonocytes [15, 19, 23].

The availability of these fermentable compounds can dictate a shift of species abundance in the gut [24]. Diets low in MACs have been shown to lead to a decrease in species abundance and overall microbial diversity, and ultimately a strong correlation with inflammation and colitis in dysbiosis [25]. Microbiome compositions among patients with inflammatory bowel disease and ulcerative colitis show significant decrease in butyrate producing microbes such as *Faecalibacterium prausnitzii* [26, 27]. The effect of consuming a high fiber diet in reducing Western diet associated disease is well accepted, however, the mechanism of action was not known. Observations by Trowell and Burkitt showed that traditional African populations were less likely to develop non-infective disease of the colon and consumed a high fiber diet [28, 29]. As new information emerges, an explanation for the protective properties of consuming a high fiber diet may point toward fermentation within the gut.

In addition to diet, the gut microbiome can be modulated via the consumption of probiotics and prebiotics. Probiotics are live organisms, typically capable of fermentation, which are consumed and survive past the stomach and reside in the small intestine [30]. Probiotics can be found in kimchi, yogurt, and other fermented foods. Prebiotics are food products which are

indigestible by the human gastrointestinal tract but can selectively increase the abundance of beneficial microbes [16, 31].

The Gut-Brain Axis

The link between gut physiology and neurologic function has been termed the "Gut-Brain Axis". The presence of certain microbes in the gut can alter physiological effects, therefore, manipulation of the gut microbiome via pre- and probiotics is a promising emerging field [32]. In particular, manipulation of the gut residents is being studied as a means of impacting behavior [33]. Depression and anxiety have also been targeted as disorders of interest [34, 35]. PKU patients may suffer behavioral, psychiatric, and neurological comorbidities in varying degrees from mild anxiolytic symptoms to phobias and psychosis at much higher rates than the general population [2, 3, 36, 37].

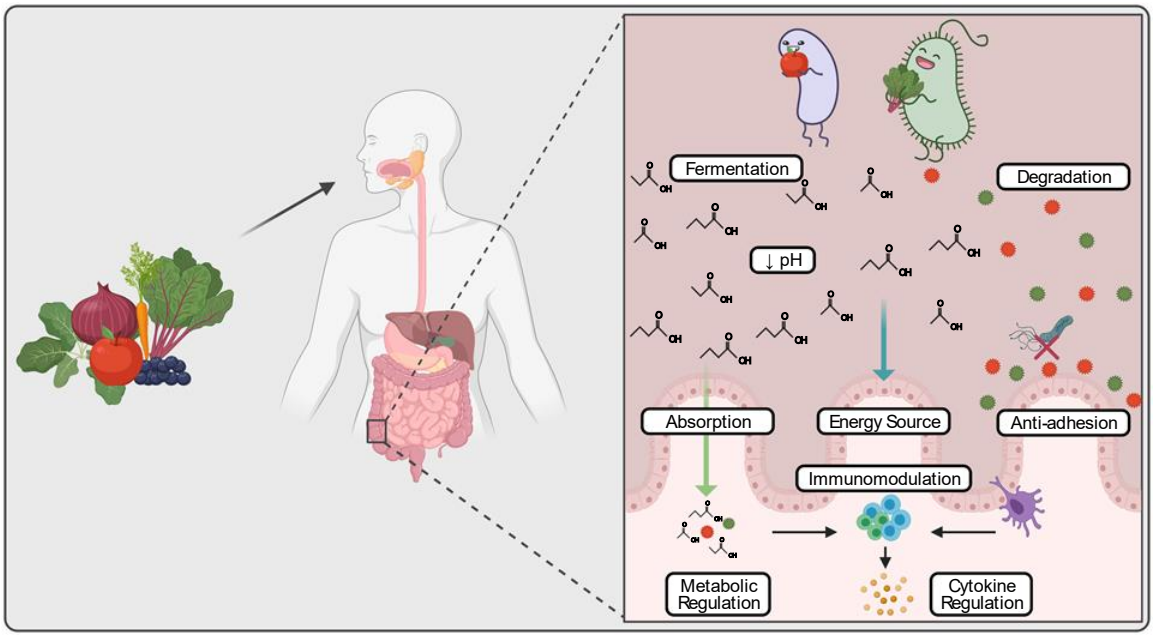

Figure 2. Fermentation of Soluble Fibers. Diagram showing the benefits of consuming fermentable fibers.

Project Overview

PKU patients often report high levels of anxiety along with symptoms of gastrointestinal distress (i.e., chronic diarrhea, constipation, cramps); symptoms previously associated with gut microbiome dysbiosis. The most common treatment for PKU is prescription of a Phe-restrictive diet, typically supplemented with an amino acid formula, the effects of which were not previously described but was suspected to be causing dysbiosis. Diet is a major factor in the composition of the gut microbiome, so a diet low in complex nutrients would be unlikely to support a robust gut microbiota. Low microbial diversity within the gut is believed to lead to the activation of inflammatory pathways and decreased resistance to pathogenic invasion [38, 39]. The primary calorie sources for PKU patients are special formula foods void of Phe and amino acid supplements [2]. The restrictive nature of the PKU treatment diet limits the intake of whole foods, and therefore microbiota-accessible carbohydrates (MACs), which encourage the growth of fermenters in the large intestine and colon [40].These beneficial commensal bacteria are major producers of butyrate, a short chain fatty acid that is capable of decreasing pH in the colon and fueling epithelial cells [41].

These studies aim to investigate the effect of the PKU treatment on the composition, diversity, and function of the gut microbiome. Additionally, we aim to test the hypothesis that a synthetic amino acid would result in gut microbiome dysbiosis, and lead to secondary changes in inflammation and behavior in mice. Preliminary mouse studies (unpublished) indicated that gut microbiome data clustered based on diet rather than genotype (i.e., PKU vs. non-PKU) (**Figure 3**), leading us to focus on diet rather than host genotype in identifying PKU related gastrointestinal problems.

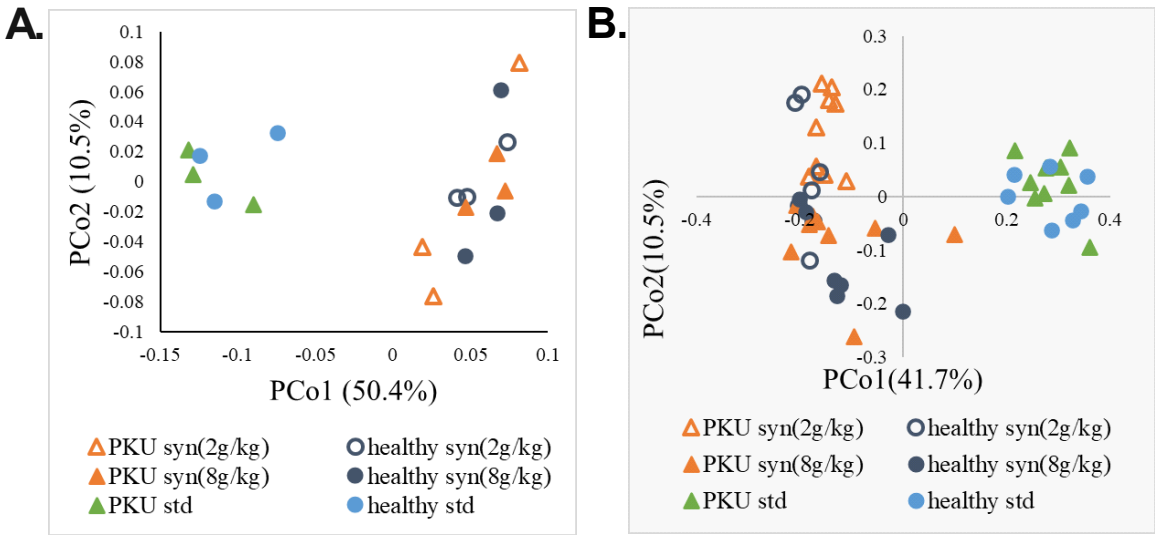

Figure 3. Sample principal coordinates analysis (PCoA) plots of weighted UniFrac distances from preliminary feeding studies. PKU and non-PKU mice were fed either a standard mouse diet, or a synthetic (free amino acids) PKU model diet with 2g/kg or 8g/kg of Phe (**A** – 2016; **B** – 2017). Each point represents samples from a single mouse and the distance between each point visually demonstrates the dissimilarity between the points. In these plots, we see a consistent clustering of the microbiome composition of mice fed the standard diet vs the mice fed a synthetic diet, regardless of Phe concentration or genotype.

Approach

Specific Aim 1: Characterize the Gut Microbiome of Phenylketonuria (PKU) Adults

Hypothesis: The gut microbiome of PKU patients differs in composition and diversity from that of healthy (non-PKU) individuals.

Stool samples were collected from PKU and non-PKU participants. DNA was extracted from the samples and the 16S rRNA gene was amplified for next-generation sequencing. The sequencing data were processed and analyzed bioinformatically to describe the adult PKU gut microbiome (**Figure 4**).

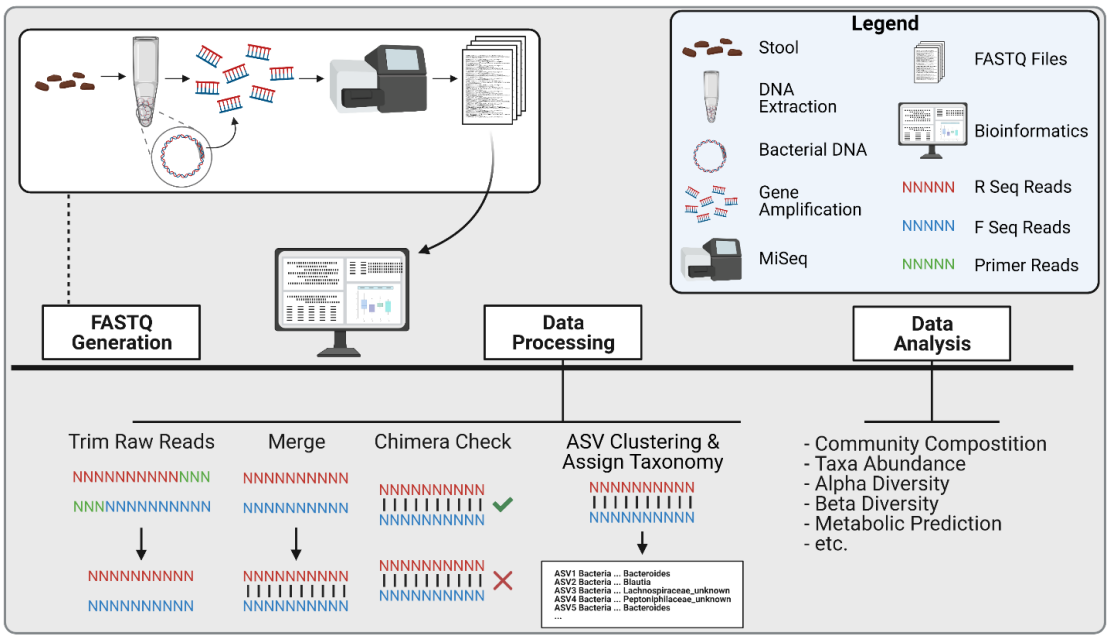

Figure 4. Microbiome analysis workflow. Bacterial DNA is extracted and amplified from stool samples. Amplicons are then sequenced to produce FASTQ files. Microbiome sequencing data are processed and analyzed.

Specific Aim 2: Determine the effects of a synthetic amino acid formula diet on microbiome dysbiosis, markers of inflammation, and behavior in mice

Hypothesis: We hypothesize that the synthetic diet will drive the gut microbiome to become less diverse, as measured by differential taxa abundance and predicted metabolic function; lead to signs of inflammation including changes in pro- and anti-inflammatory cytokines, gut morphology, SCFA production, and behavior.

Mice were randomly assigned to either the synthetic diet or standard diet feeding group at weaning. The feeding period lasted 13 weeks, meanwhile stool samples were collected weekly. At the conclusion of the 13 weeks, mice underwent behavioral tests (i.e., open field test, elevated zero maze, contextual fear conditioning). Next, animals were sacrificed, and tissues were collected for subsequent measurements to assess inflammation (**Figure 5**). Stool samples were processed and analyzed similarly to specific aim 1 (**Figure 4**).

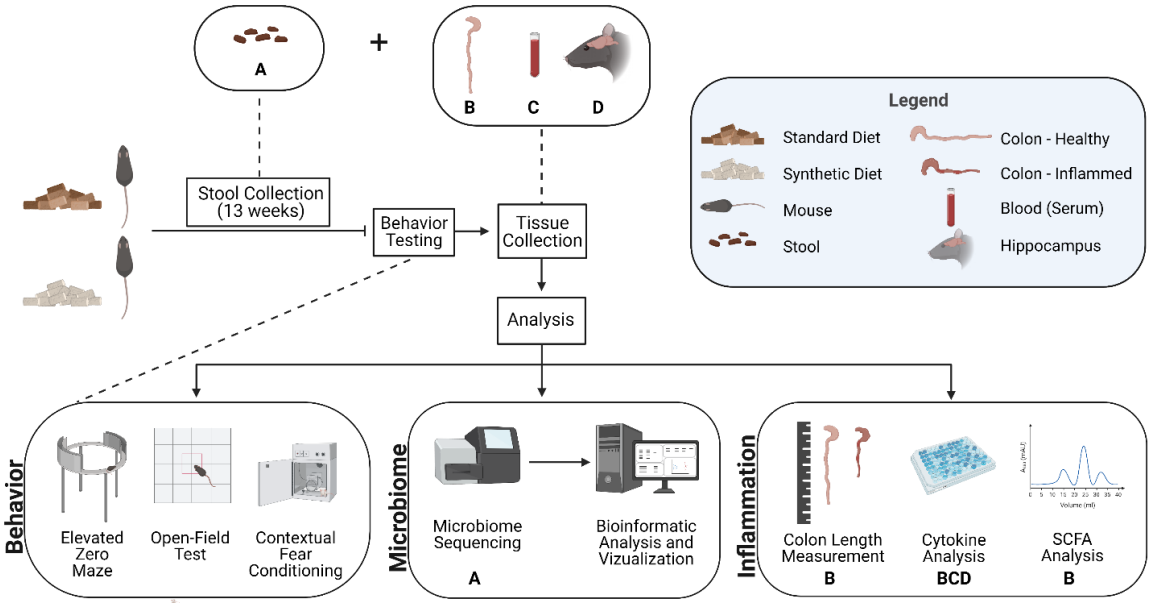

Figure 5. Interdisciplinary methodology for Specific Aim 2. Investigating the effects of consuming a synthetic formula diet on behavior, gut microbiome, and inflammation. Tissue types are denoted by illustrations described in the legend and represented by a letter beneath the assay in which they were examined (A – Stool; B – Colon; C – Blood (serum); D – Hippocampus).

Methodologies

Animals

Male C57BL/6J mice were bred in the Texas Christian University vivarium from a breeding stock obtained from Jackson Laboratory (Bar Harbor, ME). All mice received care according to the *Guide for the Care and Use of Laboratory Animals* (National Research Council, 1996), and all study protocols were approved by the Texas Christian University Institutional Animal Care and Use Committee (TCU IACUC; (#19/002). Four mice were housed under a 12-hour light/dark cycle (lights off period beginning at 1900 h) per standard polycarbonate cage (30 x 20 x 16 cm). Food and water were available *ad libitum*. All mice were weaned at postnatal day 21 and began feeding on assigned diets for a total of 13 weeks.

Microbiome Analysis

Stool samples were collected for the condition or treatment groups and control groups. DNA was then extracted from the samples and the bacterial DNA was selectively amplified. Sequencing of the 16S rRNA gene was used to obtain a snapshot of the relative abundances of microbial taxa present in a sample [42]. The gene is highly conserved, so it is often utilized as a "universal" marker for bacterial DNA and contains hypervariable regions which allow for taxa identification [43]. The V4 hypervariable region of the 16S rRNA gene was targeted in these studies.

Sequencing data were then processed, binned, and analyzed bioinformatically primarily utilizing DADA2 through R. Alpha diversity, a measure of the variation of microbes within samples groups, was calculated as a method of monitoring changes in the gut microbiome of the condition group compared to the control group. We described the richness of the samples, number of observed amplicon sequencing variants (ASVs), as well as the Shannon diversity index. Shannon diversity accounts for richness as well as diversity, which entails the distribution of ASVs among samples.

We also examined beta diversity, the variation between sample groups, through principal component analysis (PCA). We then verified that the variance between condition and control groups could be explained by our targeted condition (PKU, synthetic diet) through permutational multivariate analysis of variance (PERMANOVA) [44].

Additionally, differential taxa abundance was described between condition and control groups through DESeq2 [45]. In order to identify influential factors, or drivers for the variation between study groups, we conducted phylofactorization of the microbiome data [46].

Finally, we utilized PICRUSt2, which integrates microbiome data with open-source tools to predicted metabolic function potential of the bacteria within sample groups [47].

Inflammation

Colon length was measured as an indicator of inflammation. Following sacrifice, the digestive tract of the mouse was extracted, and we measured the length from the cecum (from the open into the colon) to the anus.

To determine if fermentation decreased along with the relative abundance of fermenting bacteria in the gut, SCFAs in the colon tissue were quantified by Microbiome Insights Inc. (Vancouver, BC, Canada) by gas chromatography (GC). Concentrations of acetate, propionate, and butyrate were assessed.

Levels of proinflammatory cytokines TNFα and IL-6, and anti-inflammatory cytokine IL-10 were quantified in the serum, hippocampal tissue lysates, and colon tissue lysates to assess inflammation using VPLEX Custom Mouse Cytokine Proinflammatory Panel 1 (mouse) multiplexing kits (Meso Scale Diagnostics, Rockville, MD).

Behavioral Analysis

Open-Field Test: The open-field test measures anxiety-like behavior, exploratory behavior, and locomotor activity in mice. Open field chambers are divided into two separate zones, including the center zone (the center of the chamber) and the outer zone (the remaining space around the center zone). Mice are individually placed in the chamber for a ten-minute period where they can roam freely. Measurements include the total duration of time spent in the center zone (seconds), total vertical counts, the total ambulatory distance traveled (centimeters), and the average speed (centimeters per second).

Elevated Zero Maze: The elevated zero maze is utilized to assess anxiety-like behavior. Mice are placed on a platform contained alternating quadrants, with two quadrants enclosed with walls and two that open. The mice are place on the platform individually and are allowed to explore for five minutes. A camera mounted above the platform measures the total distance traveled and total time spent in the open quadrants. The open quadrants are generally more aversive to mice, so less time spent in the open areas indicates more anxiety-like behavior compared to spending more time in the open areas.

Contextual Fear Conditioning: Contextual fear conditioning involves placing an animal in a novel environment and providing an aversive stimulus, and then removing it. On the following day, or testing day, the animal is placed back in the environment. Freezing indicates the animal has learned the association between the environment and the stimulus. Decreased cognition is revealed by a decrease in percent time spent freezing.

Significance and Innovation

While the gut microbiome of PKU children has been the focus of a few previous studies, we describe the gut microbiome in PKU adults for the first time [48, 49]. These findings could bolster ongoing research toward the development of a genetically engineered probiotic as a PKU therapy through gaining understanding of the adult PKU gut microbiome [50, 51].

Previous dietary studies involving the depletion of anti-inflammatory bacteria focused on the high fat content of a Western diet enabling higher lipopolysaccharide (LPS) translocation across the intestinal barrier (and into the blood stream), with little emphasis on the role of reduced levels of complex carbohydrates on the microbiome [52]. Given the known ability microbiota in eubiosis to enhance tight junction function of the intestinal epithelial cells by the production of SCFAs (via fermentation of resistant starches), it is possible that a large portion of the LPS

translocation may be from the loss of fermenters on the Western diet, independent of dietary fat intake [53-57]. Additionally, a mouse model has demonstrated influence between blood-brain barrier permeability and the gut microbiota, signaling the additional impact of diet on neuropsychological comorbidities [58].

If the conventional PKU treatment diet shows similar inflammatory changes to the Western diet such as heightened inflammatory cytokines despite being a low-fat diet, it could change our understanding of how diet and microbiome may modulate inflammatory status. Dietary intake of prebiotics (ex. fructooligosaccharides, apple pectin, inulin, etc.) have been shown to have positive impact on the abundance of butyrate producing bacteria [4]. These interdisciplinary findings could support a paradigm shift in the way we view diet, by focusing on foods that promote microbiota health, as opposed to most diet regimens that only focus on what not to eat.

CHAPTER II

THE ADULT PHENYLKETONURIA (PKU) GUT MICROBIOME

Phenylketonuria (PKU) is an inborn error of phenylalanine metabolism primarily treated through a phenylalanine-restrictive diet that is frequently supplemented with an amino acid formula to maintain proper nutrition. Little is known of the effects of these dietary interventions on the gut microbiome of PKU patients, particularly in adults.

In this study, we sequenced the V4 region of the 16S rRNA gene from stool samples collected from adults with PKU (n = 11) and non-PKU controls (n = 21). Gut bacterial communities were characterized through measurements of diversity and taxa abundance. Additionally, metabolic imputation was performed based on detected bacteria.

Gut community diversity was lower in PKU individuals, though this effect was only statistically suggestive. 65 genera across five phyla were statistically differentially abundant between PKU and control samples ($p < 0.001$). Additionally, we identified six metabolic pathways that differed between groups ($p < 0.05$), with four enriched in PKU samples and two in controls.

While the child PKU gut microbiome has been previously investigated, this is the first study to explore the gut microbiome of adult PKU patients. We find that microbial diversity in PKU children differs from PKU adults and highlights the need for further studies to understand the effects of dietary restrictions.

Introduction

Phenylketonuria (PKU, OMIM 261600), is a genetic disorder characterized by dysfunctional metabolism of the essential amino acid phenylalanine (Phe) and occurs in approximately 1 in 10,000 births per year worldwide [59]. Disrupted phenylalanine metabolism can be caused by an autosomal recessive mutation in the *PAH* gene, resulting in a dysfunctional phenylalanine hydroxylase (PAH), or lack of its cofactor tetrahydrobiopterin (BH4) [60]. When dietary Phe is consumed in a healthy system, it is absorbed in the gut and transported through the blood to the liver where it is metabolized to tyrosine by PAH. In PKU patients, lack of functional PAH or BH4 leads to the accumulation of Phe and its derivatives in the blood. If left untreated, accumulation can reach neurotoxic levels, and result in increased incidence of developmental problems including intellectual disabilities, growth failure, and seizures.

Worldwide, newborns undergo routine screenings for several disorders, including PKU [61]. Upon detection of above-average concentrations of phenylalanine in the blood, an infant will proceed to further testing in order to determine a diagnosis for PKU. Typically, Phe concentrations range from 1.3 to 2.0 mg/dL in the blood, but in classic PKU blood Phe concentrations can exceed 20 mg/dL [62]. Immediately after diagnosis, the infant is prescribed a phenylalanine-restricted diet supplemented with an amino acid formula. Although this is currently the most effective and only universal treatment for PKU, Phe is an essential amino acid found in most complex proteins and whole foods. Therefore, the PKU diet can be low in protein, fiber, and other important nutritional sources; thus, leading to difficulty in patient compliance and nutritional deficiencies [3, 62]. Nutritional deficiencies include but are not limited to vitamin B12, iron, and long-chain fatty acids [63-65].

Active research and developments aim to provide patients with alternative treatment options for PKU. Of note, a recent study found that inhibition of SLC6A19, a neutral amino acid transporter, led to decreased Phe in plasma and increased urinary excretion of Phe [66]. Enzyme replacement therapy aims to reduce Phe through the use of enzymes capable of metabolizing Phe, for example, rAvPAL-PEG (PEGylated recombinant phenylalanine ammonia lyase) which transforms phenylalanine to ammonia and trans-cinnamic acid [67]. Additionally, probiotics have been engineered to express phenylalanine-metabolizing enzymes upon oral administration by the host [50, 51]. Administration of PAL as a therapeutic option has previously proved to be difficult due to issues with stabilization and high cost; however, the probiotic provides protection from stomach acids, allowing for the enzymes to be expressed later in the digestive tract where it can become metabolically active, ultimately reducing Phe in the host [68].

The gut microbiome is a complex collection of microbes housed primarily in the colon and has been found to influence the physiology of distal organs through association with diseases such as type 2 diabetes, inflammatory bowel disease (IBD), asthma [69-71]. Gut microbiome activity has been suggested to alter blood-brain barrier permeability and has also been linked to psychiatric disorders including autism, schizophrenia, and anxiety [58, 72-74].

The composition of the gut microbiome is affected by many factors including medications, birth route (vaginal or cesarian), and host genetics, but is primarily shaped by diet [5, 31]. Previous studies have investigated the impact of the PKU treatment diet and Phe restriction on children and have found notable differences in the gut microbial community as compared to non-PKU controls [48, 49]. Though these studies document the impact of PKU treatment in children, little is known about the impact of the PKU diet in adults. While the development of a probiotic for the treatment of PKU is a promising approach, little is known about the baseline community of the gut

microbiome of PKU patients over the entire lifespan; the composition of which has direct implications on the success or impact of any therapeutic probiotic that becomes available [75]. In this study, we examine the gut microbiome of 32 adults with and without PKU using a 16S rRNA gene fragment metabarcoding approach.

As the PKU diet is extremely restrictive and characteristically different than that of the general population, we expected the composition of the PKU treated gut microbiome to be markedly different from the control group in both diversity and taxonomic composition, with subsequent changes in metabolic capacity and activity. To our knowledge, this is the first study to catalog the gut microbiome of adults with PKU. Characterization of the PKU adult gut microbiome may prove beneficial to the development of new therapeutics or improvement of treatment options currently available.

Materials and Methods

Sample Collection

A total of 32 (11 PKU, 21 non-PKU controls) stool samples were collected by participants using a Puritan HydraFlock® swab in DNA/RNA Shield (Puritan Medical Products, Guilford, ME, USA), returned to lab personnel, and stored at -20°C until ready for DNA isolation and quantification.

The average age of control subjects was 29 years (± 3.07). Both control and PKU samples were collected from approximately equal numbers of males and females. Average age of PKU subjects was 33 years (± 1.98). Control samples were collected from 11 females and 10 males, PKU samples from 4 females, 6 males, and 1 N/R (sex not reported by one participant) (Table 1).

The study was approved by The North Texas Regional Institutional Review Board (IRB Protocol#2018-114 and #2018-193).

Table 1. Baseline characteristics of the subjects.

Observations	**PKU (*n* = 11)**	**Control (*n* = 21)**
Sex		
Female	4	11
Male	6	10
N/R[1]	1	0
Average Age (years)	33 ± 1.98	29 ± 3.07

[1] N/R: not reported by participant

DNA Isolation and Quantification

Fecal samples were thawed on ice and DNA was extracted using the Kingfisher MagMAX Microbiome Ultra Nucleic Acid Isolation Kit (Thermo Fisher Scientific, Waltham, Massachusetts) following the manufacturer's protocol the final elution volume was adjusted to 50µl. The extracted DNA was quantified using a NanoDrop1000 spectrophotometer (ThermoFisher Scientific Inc., Waltham, MA, USA) and stored at -20°C.

16S rRNA Gene Amplification

The V4 hypervariable region of the 16S rRNA gene was amplified in duplicate from the previously extracted DNA utilizing illumv4_515F (5' – GTGCCAGCMGCCGCGGTAA – 3') and illumv4_806R (5' – GGACTACHVGGGTWTCTAAT – 3') primers with Illumina sequencing adaptors [43]. PCR reactions were prepared in 25µl volumes consisting of 2.5 µl 10× Accuprime™ PCR Buffer II (Invitrogen, Carlsbad, CA), 0.5 µl forward and reverse primer (10 µM), 0.1 µl of Accuprime™ Taq DNA Polymerase High Fidelity (5U/µl), 1 µl of template DNA (10-100ng), and 16.9 µl molecular grade water. Negative and positive controls were produced

along with every master mix containing either 1-µl *Escherichia coli* genomic DNA or 1 µl of molecular grade water, as appropriate. Thermocycler conditions included an initial annealing at 94°C for 2 minutes followed by 30 cycles of 94°C for 30 s, 55°C for 40 s, 68°C for 40 s, and a final extension at 68°C for 5 minutes. PCR products were visualized on a 1% agarose gel. Bands were observed in all positive PCR controls and absent for all negative controls.

Library Preparation and Sequencing

Duplicate PCR products were pooled into a single tube and purified using Agencourt® AMPure® XP magnetic beads (Beckman Coulter) following the manufacturer's instruction. Purified samples were then dual indexed using the Nextera XT assay to allow for multiplexing. The 50 µl PCR recipe and thermocycler protocol were as follows per sample: 5 µl 10x Accuprime™ PCR Buffer II, 5 µl Nextera XT Index Primer 1, 5 µl Nextera XT Index Primer 2, 0.2 µl, Accuprime™ Taq DNA Polymerase High Fidelity, 5 µl DNA (~10 pm DNA), and 29.8 µl of molecular grade water; initial denaturation at 94°C for 3 minutes, 8 cycles of 94°C for 30 s, 55°C for 30 s, 68°C, and a final extension at 68°C for 5 minutes. Labeled products were purified as previously described by AMPure® XP magnetic beads and quantified using the Qubit® 2.0 fluorometer (Invitrogen, Carlsbad, CA). Following quantification, libraries were pooled at equimolar concentrations and then diluted and denatured for a final concentration of 10 pM. . The product was loaded into the MiSeq Reagent Kit v2 cartridge (Illumina Inc, San Diego, CA) and sequenced on the Illumina MiSeq® instrument, along with an internal control sample consisting of 5% PhiX DNA, for paired-end high-throughput sequencing at 500 cycles.

Sequencing Data Analysis

Primers were trimmed from raw reads using Cutadapt v. 1.16 [76]. Trimmed reads were quality filtered, merged, checked for chimeras, and clustered into Amplicon Sequencing Variants (ASVs) using the DADA2 pipeline [77]. Finally, taxonomy was assigned to processed sequences using VSEARCH v. 2.8.1 and the EzBiocloud database as a reference . Data analysis was primarily performed within the R version 3.5.0 environment [78, 79]. Alpha diversity was calculated using phyloseq v. 1.30.0 [80]. Beta diversity was calculated using PhILR transformed data and the Vegan v. 2.5-5 library [81, 82]. Analysis of variance was determined via permutational multivariate analysis of variance (PERMANOVA) [44]. Differential abundance of specific bacteria or phylogenetic clades between PKU positive and control samples was calculated with DESeq2 and Phylofactor [45, 46]. To predict differences in the metabolic potential between the PKU gut microbiome compared to the control gut microbiome we utilized the PICRUSt2 (Phylogenetic Investigation of Communities by Reconstruction of Unobserved States) pipeline [47]. Visualization of metagenome imputation was then completed with STAMP (STatistical Analysis of Metagenomic Profiles) [83]. The script for all read processing, analyses, and visualization can be accessed at https://github.com/vivmancilla/PKU_adults.

Results

Gut Microbial Composition of PKU Patients Diverges from Control Individuals

Five bacterial phyla were detected in both the PKU and control groups (based on a >1% abundance). Firmicutes was the predominant bacterial phyla in both PKU (63.55 ± 12.88%) and control cohorts (68.15 ± 12.86%) (Figure 1). Bacteroidetes was the second most abundant

population in both PKU (30.55 ± 9.86%) and control cohorts (25.57 ± 13.19%) followed by Actinobacteria, Proteobacteria, and Verrucomicrobia (<10%).

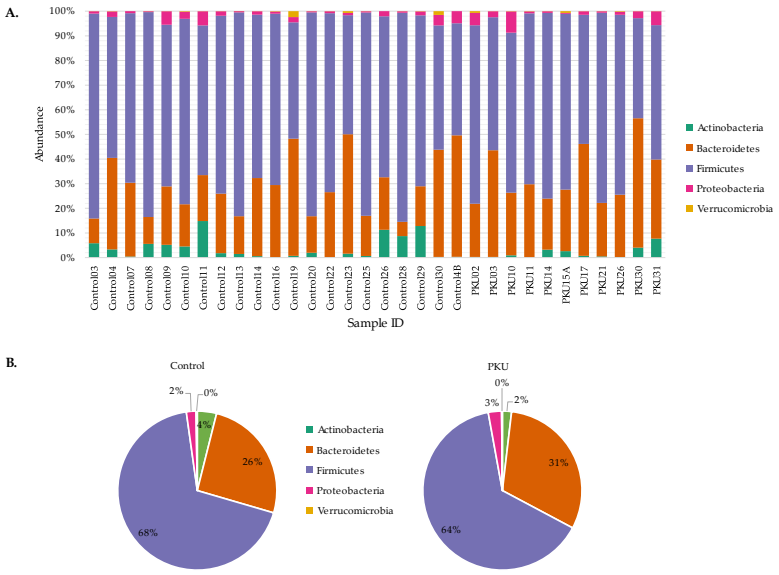

Figure 1. Phylum level comparison between PKU and control samples. Stacked histogram (**A**) and pie graph (**B**) representing the individual and average abundance of phyla (>1% relative abundance) in PKU and control samples.

To identify specific groups or clades of bacteria that were predictive of PKU status, we ran two separate analyses, DESeq2 and Phylofactor [45, 46]. While the motivation for running these analyses are the same, DESeq (ASV-based pairwise comparison) identifies broader differences in taxa abundance between PKU and control samples while Phylofactor searches for potential bioindicators of PKU.

DESeq2 identified 65 differentially abundant genera ($p < 0.001$) in PKU compared to control samples (Figure 2). Genera enriched in PKU samples include *Bifidobacterium*, *Bacillus*, *Alistipes*, *Clostridium*, *Akkermansia*, and *Bacteroides*. Alternatively, genera decreased in PKU samples include *Lactobacillus*, *Porphyromonas*, *Frisingicoccus*, *Blautia*, and *Faecalibacterium*.

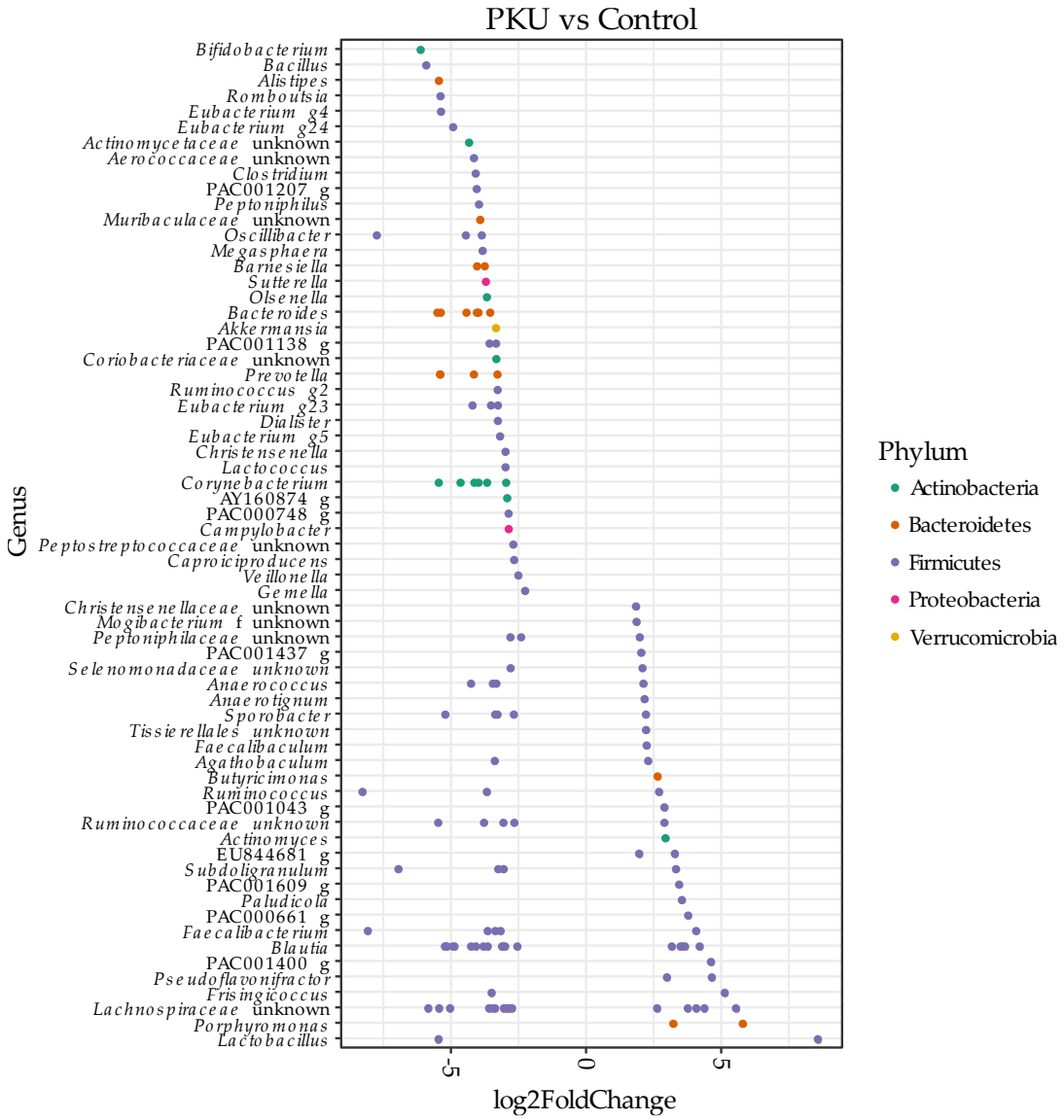

Figure 2. Pairwise comparison (DESeq2 analysis). Differentially abundant ASVs ($p < 0.001$) in PKU patients and non-PKU control counterpart samples are shown. ASVs were assigned to the genus (y-axis) and phylum level (colors). Negative "log2 Fold Change" values (x-axis) indicate higher abundance in PKU samples and positive values indicate higher abundances in control samples.

Phylofactor analysis, or '"phylofactorization", of all bacterial ASVs present in the PKU and control dataset identified three phylogenetic factors influencing microbial community composition (Figure 3) [46]. F-statistics identified "bioindicator" clades between conditions

(Figure 3a). Clades of interest for PKU in comparison to control samples included: *Romboustia* (green; W = 19, *p* = 3.049e-05) lower in PKU samples (Figure 3b), Lachnospiraceae (purple; W = 47, *p* = 0.005567) lower in PKU samples (Figure 3c), and *Enterocloster* (formerly classified as *Clostridium* in EZBioCloud database [84]) (orange; W = 192, *p* = 0.001691) higher in PKU samples compared to control samples (Figure 3d).

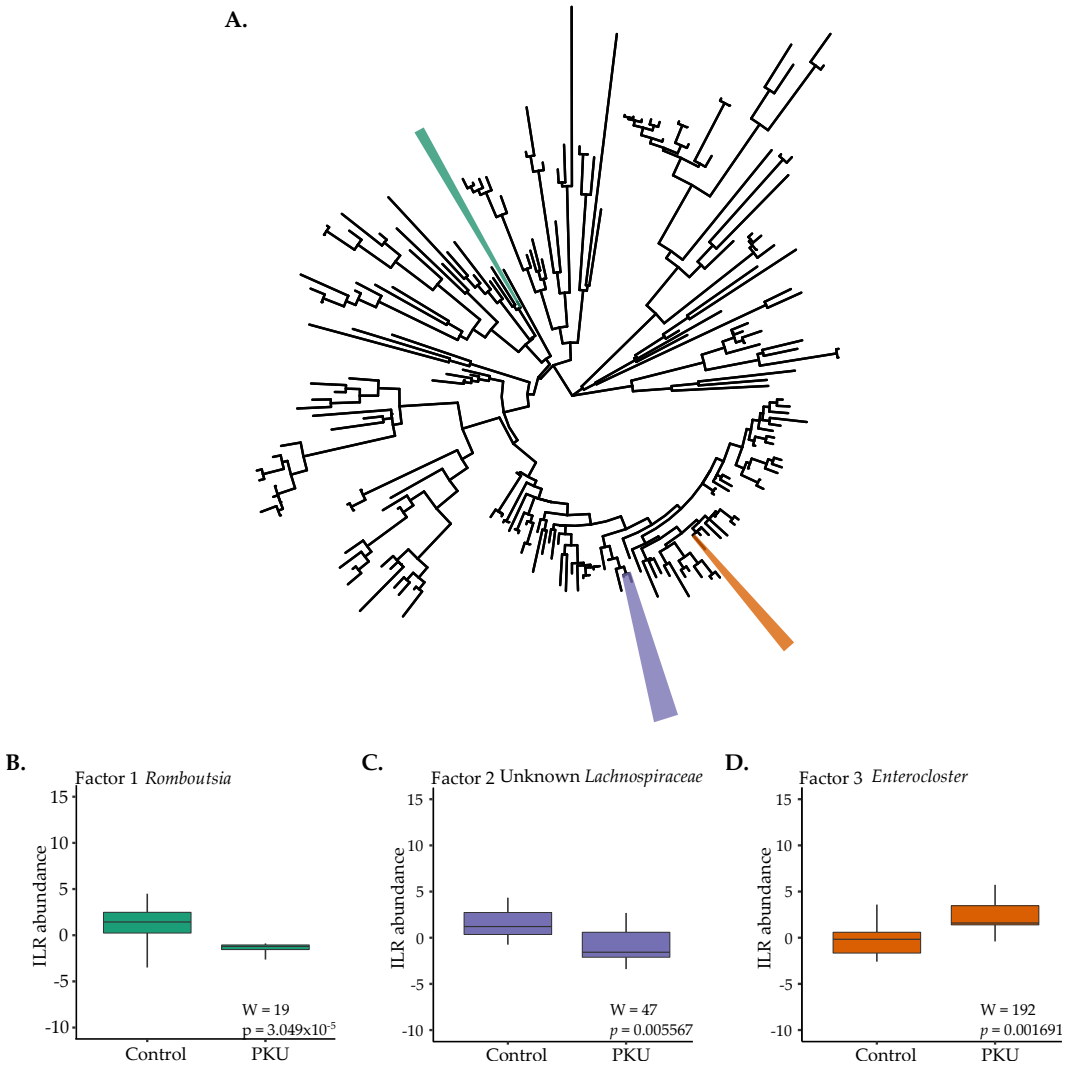

Figure 3. Phylofactorization of all bacterial ASVs present in PKU and control fecal samples (**A**). Three factors were identified as the most influential members differentiating PKU and control samples at the genus level: (**B**) *Romboustia* (green), (**C**) two unknown *Lachnospiraceae* (purple), and (**D**) *Enterocloster* (orange).

Comparison of Microbial Diversity of PKU and Control Samples

Alpha diversity, the variation of microbes within sample groups, was estimated with both ASV richness (Figure 4a) and Shannon diversity index (Figure 4b). Richness was measured by a count of distinguishable ASVs in each sample group. Shannon diversity index accounts for the richness and diversity (distribution of ASV abundance) of the sample groups. Adult PKU patients had lower, but not statistically significant differences in microbial diversity as measured by both the number of observed ASVs (Wilcoxon: W=143, p-value=0.28) and Shannon index (Wilcoxon: W=139, p-value=0.37).

Beta diversity, the variation of microbial communities between sample groups, was estimated by way of Principal Component Analysis (PCA) of Phylogenetic Isometric Log-Ratio (PhILR) transformed distances for PKU and control samples (Figure 5). PhILR utilizes a phylogenetic approach to transform microbiome data in order to produce coordinates which can then be used to produce PCA plots [81]. In PCA plots, individual points represent compressed data found for individual samples and located based on dissimilarity of microbial communities. Analysis of the variance of the "data cloud"of each sample group through PERMANOVA determined that the differences in impact of samples based on group (PKU vs control) were statistically significant (R^2=0.06, p-value=0.02); though this only explained about 6% of the total diversity [44].

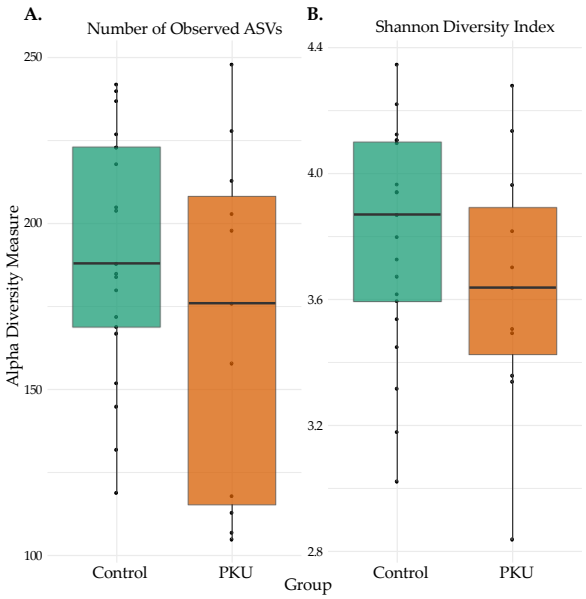

Figure 4. Alpha diversity for PKU and control samples. Statistical significance of the (A) number of observed ASVs and (B) Shannon diversity index from PKU and control samples were calculated and compared with the Wilcoxon rank-sum test. Median scores are represented with a horizontal line, the box outer limits represent the first to third quartiles, the whiskers indicate the range of measurements for each group, and each point denotes a sample. Observed ASVs (Wilcoxon: W = 143, p = 0.28) and Shannon index (Wilcoxon: W = 139, p = 0.37).

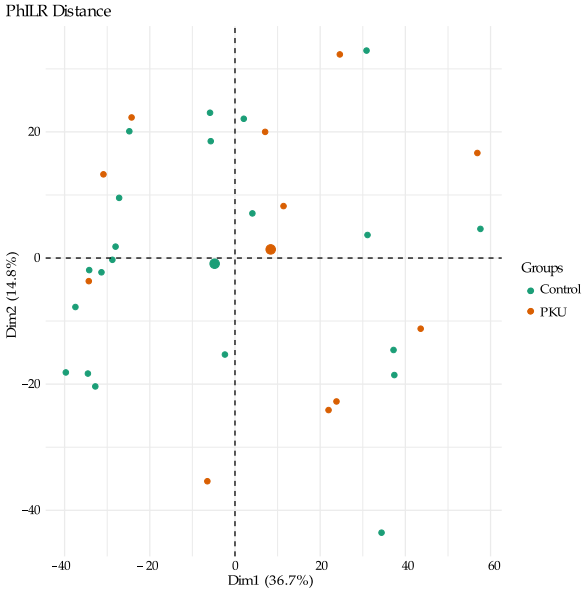

Figure 5. Genus-level beta diversity comparison of the gut microbiota compositions. Based on principal component analysis (PCA) of PhILR distances for PKU (orange) and control (green) samples. Each point represents a sample, and the condition is denoted by its color; larger circles represent the mean coordinates for each group.

Metagenome Imputation Analysis

To predict the effect of PKU on the metabolic function of the gut microbial community compared to that of controls, we performed PICRUSt analysis, the results of which were visualized with STAMP (Figure 6) [47, 83]. 16S marker sequences of bacteria identified in PKU and control samples along with open-source tools were integrated by PICRUSt2 in order to predict functional potential of the PKU gut microbiome and the control gut microbiome.

Significance ($p < 0.05$) was found in six MetaCyc pathways; four pathways were enriched in the PKU samples (Biotin Biosynthesis II, Superpathway of N-acetylneuraminate Degradation, Allantoin Degradation to Glyoxylate III, Gluconeogenesis I) and two pathways were decreased in PKU samples (Creatinine Degradation II, Superpathway of 2,3-butanediol Biosynthesis).

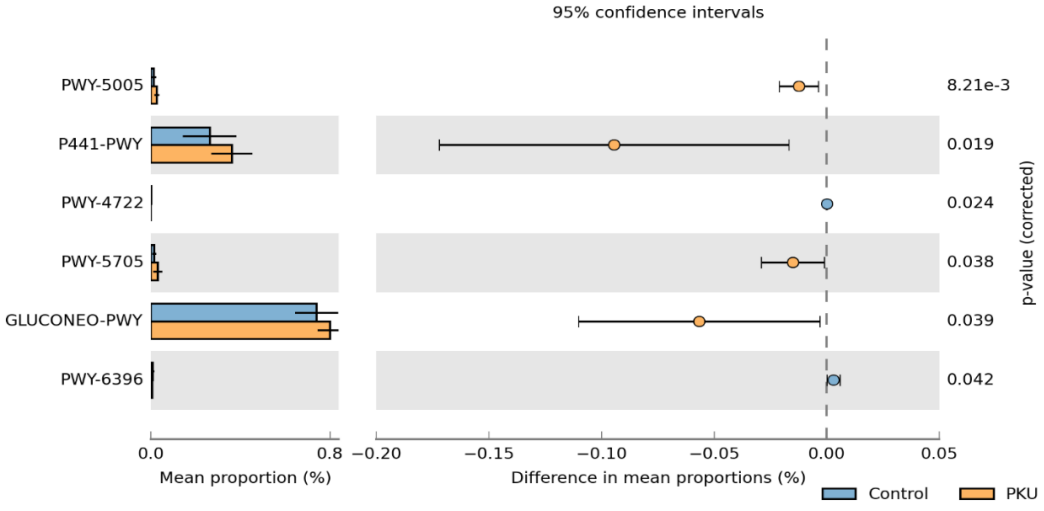

MetaCyc Pathways

PWY-5005	Biotin Biosynthesis II
P441-PWY	Superpathway of N-acetylneuraminate Degradation
PWY-4722	Creatinine Degradation II
PWY-5705	Allantoin Degradation to Glyoxylate III
GLUCONEO-PWY	Gluconeogenesis I
PWY-6396	Superpathway of 2,3-butanediol Biosynthesis

Figure 6. The relative abundance of predicted microbial genes related to metabolism in control (blue) and PKU (orange) samples was based on Welch's t-test ($p \leq 0.05$). The colored bars represent 95% confidence intervals calculated using Welch's inverted method. The colored circles represent the difference in mean proportions between PKU and control samples.

Discussion

In this study, we sequenced the V4 hypervariable region of the 16S rRNA gene from stool samples collected from adult PKU and non-PKU control individuals. In order to understand the effects of PKU on the gut microbiome we explored the gut microbial community composition, diversity, and predicted changes in metabolic potential in relation to non-PKU controls.

Broadly examining the gut microbial composition at the phylum level, Bacteroidetes and Firmicutes dominate the population in both the PKU and control samples, followed by Actinobacteria, Proteobacteria, and Verrucomicrobia (Figure 1). There is currently no consensus on phylum level comparisons between previous studies involving children with PKU and no prior studies have been published on the gut microbiome of adults diagnosed with PKU [48, 49]. We then took a genus level approach to describe relative abundance and identify potential bioindicators of PKU with DESeq2 and Phylofactor respectively.

DESeq2 analysis found 65 genera were significantly differentially abundant (Figure 2). Of note is *Faecalibacterium*, which was shown here to be decreased in PKU adult samples and has been reported in previous studies investigating PKU children [48, 49]. *Faecalibacterium* consume dietary fiber found in whole foods and produce short chain fatty acids (SCFA), mainly butyrate which acts as a pH buffer and primary source of energy for colonocytes [85]. These bacteria possess anti-inflammatory properties through production of butyrate and Microbial Anti-Inflammatory Molecule (MAM [23, 86-88]. Interestingly, Crohn's disease, IBD, and colitis patients are among several groups found to also contain lower levels of *Faecalibacterium* in stool samples [89-91]. As previously mentioned, the PKU diet can be low in protein, whole foods, and fiber. Conversely, the "Western Diet" largely consists of processed, high fat, high protein foods, yet those consuming this diet house a gut microbiome also low in the beneficial, fiber degrading

microbes such as *Faecalibacterium* [52]. Future studies may investigate similar properties of these opposing diets to determine the factor responsible for decreased abundance of beneficial, anti-inflammatory microbes.

Phylofactorization of microbiome data from PKU and control samples revealed three factors to be influential at the genus level (Figure 3): *Romboustia*, 2 unkown Lachnospiraceae genera, and *Enterocloster*. Currently, the specific roles that *Romboustia* and *Enterocloster* are largely unknown due to recent isolations and classifications, however, further studies of the bacteria may expose the importance of their presence [84, 92]. Potentially relevant to PKU is that isolated *Romboustia* genera lack a catalytic enzyme for the biosynthesis of phenylalanine and tyrosine [93]. Alternatively, Lachnospiraceae make up the core human gut microbiome and abundance variations span several diseases and disorders linked to gut dysbiosis, leading to inconsistent conclusions in the role the microbe may play [94].

Ecological diversity was determined by several measures of alpha and beta diversity. Alpha diversity was considered through observed ASV counts and calculation of the Shannon diversity index. Previous studies by Bassanini et al. and Pinheiro de Oliveira et al. reported significantly decreased alpha diversity in stool samples from PKU children compared to non-PKU children [48, 49]. In this study we found that while alpha diversity similarly trended lower in PKU adults, the effect was not significant. Further investigation is necessary to determine if the PKU diet and treatment has a more pronounced impact on the gut microbiome of children, which is still developing and not as stable as the adult gut microbiome [95]. Alternatively, differences in microbial diversity between PKU children and adults may be a function of a more regulated diet in children as typically parents are planning meals and maintaining a sense of stability, which may

lead to better adherence to the diet and subsequently a more dramatic drop in gut microbial diversity. Adults with PKU, on the other hand, may deviate more often from the prescribed diet.

Dysbiosis is often defined by alterations or deviance from "normal" or "healthy" microbiota and often associated with disease [14]. In order to determine if the PKU gut microbiome profile was significantly deviated from that of non-PKU controls, we performed a PERMANOVA. Results verified a significant difference between the two groups. PKU patients often experience comorbidities spanning multiple organ systems including autoimmune, gastrointestinal, and neuropsychiatric disorders; some of which have been associated with dysbiosis [36, 37, 96]. Further studies are necessary to determine if the variances described here can be implicated in PKU comorbidities.

As previously mentioned, gut microbiome composition can be shifted through extrinsic mechanisms such as diet, medication, and environment; however, microbiome influence can be bidirectional in that gut microbiota shifts have been shown to contribute to changes in the immune system and even mood and cognition through the gut-brain-axis [97, 98].

Finally, we found significant differences in predicted metabolic pathways between PKU positive individuals on a Phe-restrictive diet and control individuals. Pathways that were upregulated in PKU patients included those involved in carbon fixation and carbohydrate fermentation. Interestingly, N-acetylneuraminate degradation was found to be higher in PKU patients; a pathway that previously has been identified as an important factor for pathogenic bacterial proliferation and permeation into the blood stream in immunocompromised individuals [99]. Identification of pathways that impact the pathogenicity of bacteria may shed light on the higher susceptibility of PKU patients to infectious diseases—including gastroenteritis, colitis, urticaria, rhinitis, and tonsillitis—as compared to the general population [96, 100]. Though these

imputations are limited, they highlight the need to further explore the effect of the PKU diet on PKU patients through multiple angles, including metabolomics and transcriptomics.

Although the current diet-based treatment is effective at maintaining low Phe levels, the impact of the PKU diet and treatment over the course of a patient's lifetime remains an unknown. As the gut microbiome can affect distal organs and systems, it is important to fully characterize the impact of this treatment on the gut microbiome in PKU patients.

In this study, we detected significant differences in the abundance of specific bacterial groups and putative metabolic pathways in adult PKU patients as compared to control individuals. Unlike the previous studies of PKU children, we did not find significant differences in diversity of the gut microbiome. The results of this study illustrate the need for further studies with larger samples sizes and representation (i.e., sex and race) to understand the full effects PKU dietary restrictions and treatments have on patients over time.

CHAPTER III

A SYNTHETIC FORMULA AMINO ACID DIET LEADS TO MICROBIOME DYSBIOSIS, REDUCED COLON LENGTH, AND SECONDARY MARKERS OF INFLAMMATION IN A MURINE MODEL

The gut microbiome is a collection of microbes residing primarily in the large intestine. The colon is a major production site for short chain fatty acids (SCFAs) through anaerobic fermentation by commensal bacteria. SCFAs provide a source of energy for the colonocytes, as well as provide anti-inflammatory benefits. The production of SCFA appears to be dependent on the availability of soluble fibers and members of the gut microbiota capable of fermentation.

In this interdisciplinary study, we monitored the effect of a consuming synthetic diet on the composition of the murine gut microbiome over the course of 13 weeks, beginning at weaning. At the conclusion of the feeding period, mice we observed for anxiolytic behavior, locomotion, and cognition. We also searched for markers of inflammation through colon shrinkage, changes in cytokine levels within several tissues, and determined the concentration of SCFAs in the colon at the conclusion of the feeding period.

The gut microbiome of mice fed the synthetic diet experienced significant deviation from the control group which affected relative abundance of beneficial bacteria. Mice on the synthetic diet were found to have shorter colons, lower concentration of SCFAs in the colon, and demonstrated elevated exploratory behavior.

Introduction

The gut microbiome plays a variety of fundamental roles in health and disease such as protecting against opportunistic pathogens, extracting nutrients and energy from our diets, and helping maintain normal immune function [101-104]. It is known to impact distal organs and systems such as the brain(through the gut-brain axis) and immune function by microbial signaling and metabolites including SCFA [32-34, 87, 105-109]. Factors including age, genetics, and diet can influence gut microbiome composition [110].

Alterations to diet can dramatically influence human health. Unraveling the interrelations between diet, health and the gut microbiota can have major implications for disease and disorder treatment, as well as general wellness. Sudden changes in diet have been shown to shift the community structure of the microbiota within a single day, change the representation of metabolic pathways in the microbiome, and alter microbiome gene expression [5]. Mammalian gut microbiomes are thought to share a functional "core" community, but there is a variable community as well that can be changed by environmental stimuli, such as diet [111].

Diet is a primary driver of gut microbiome composition, fiber intake in particular, is dietary modification that dramatically and reproducibly affects gut microbiome composition. Recent research has shown, for example, that people who switch between plant- and meat-based diets or people who add more than 30 grams per day of dietary fibers to their diet could dramatically alter the composition and function of their gut microbiota in a matter of days [112, 113].

Dietary fiber is a source of microbiota-accessible carbohydrates (MACs). Consumption of a complex diet with many complex carbohydrates results in increased gut epithelial health and increased microbiota diversity. Conversely, if fiber consumption is low, then gut microbes will

lack access to complex carbohydrates, resulting in decreased diversity and a potential shift from commensal microbiota to dysbiosis [40]. One reason for this appears to be related to the intestinal mucosal barrier. For instance, it has been shown that a low-fiber diet promotes the expansion and activity of colonic mucous-degrading bacteria, which results in the erosion of the colonic mucosal barrier, increasing the risk of opportunistic infections [114]. Diet not only influences the composition of the gut microbiome, but it also affects microbial metabolism, which in turn can influence host health [115].

High-fiber diets provide nutrients to obligate anaerobes in the colon which then produce short-chain fatty acids (SCFAs) such as butyrate, propionate, and acetate [15]. These SCFAs are then metabolized by colonocytes in a way that results in high oxygen consumption, thus maintaining epithelial hypoxia, favoring the growth of the same commensal obligately anaerobic SCFA producers [116]. Low-fiber diets, on the other hand, fail to support SCFA producers in the gut, thus starving gut epithelial cells of these energy sources, and resulting in higher levels of anaerobic glycolysis, which is characterized by high lactate release and low oxygen consumption. Under these conditions, epithelial hypoxia cannot be maintained, and facultative anaerobes begin to flourish in the gut, resulting in dysbiosis and inflammation [116].

Recently several groups have linked microbiota-generated SCFAs to anti-inflammatory effects. SCFAs increase the pool of regulatory T cells in the gut and are protective against allergic airway inflammation in a mouse model [107, 117]. In a study with ulcerative colitis patients, mucosal levels of pro-inflammatory cytokines were reduced by administration of butyrate and this correlated with a decrease in disease pathology [118]. Other studies have found that decreased levels of SCFA-producing microbes in the gut is associated with colonic disease, including inflammatory bowel disease (IBD) [27, 119]. Based on this understanding, SCFAs appear to

provide direct anti-inflammatory benefits to the gut environment and help maintain a protective barrier to prevent diseases like IBD. Additionally, in a recent study, children diagnosed with phenylketonuria (PKU) were found to have decreased levels of fecal butyrate associated with a restrictive low-Phe diet along with Phe-free amino acid formula supplementation, despite consuming soluble fiber [120]. PKU children were compared to children diagnosed with mild hyperphenylalaninemia (MHP), therefore, while MHP children are affected by PKU, they are not on a Phe-restrictive diet. The authors also describe the children's gut microbiota as being depleted in *Faecalibacterium prausnitzii* and *Roseburia* spp. *F. prausnitzii* abundance has previously been shown to be positively associated with fecal butyrate content [121]. This raises the question of what aspect of the Phe-restrictive diet may be contributing to the inhibition of fermentative gut bacteria. In this study, we focus on the impact of a synthetic, free-amino acid diet analagous to that prescribed for PKU patients (but without specific Phe restriction) on the gut microbiome, inflammation, and behavior in a wild type mouse model. Specifically, we fed two groups of mice either a diet of standard chow or a synthetic diet version in which all complex proteins were replaced with equivalent levels of free amino acids for a period of 13 weeks. Additional nutritional information in APPENDIX A-D.

Over the course of the study, we assessed the microbial composition of their gut microbiome and investigated possible changes in behavior. Finally, we assayed multiple tissues for changes in cytokine markers of inflammation, SCFA levels, and impacts on colon length.

Methods & Materials

Experimental Design

Male C57BL/6J mice bred in the Texas Christian University vivarium from a breeding stock obtained from Jackson Laboratory (Bar Harbor, ME) were utilized for this experiment. All mice received care according to the *Guide for the Care and Use of Laboratory Animals* (National Research Council, 1996), and all study protocols were approved by the Texas Christian University Institutional Animal Care and Use Committee (TCU IACUC; (#19/002). Four mice were housed under a 12-hour light/dark cycle (lights off period beginning at 1900 h) per standard polycarbonate cage (30 x 20 x 16 cm). Food and water were available *ad libitum*. All mice were weaned at postnatal day 21. Following weaning, animals were assigned to two groups based on the standard mouse diet (n = 10), Prolab RMH 1800 (LabDiet, St. Louis, MO), or the synthetic formula diet (n = 10), TD 190275 Amino Acid Diet (5LL2) (Envigo Teklad Diets, Madison, WI) for 13 weeks (**Figure 1**). The synthetic diet was developed to mimic the standard diet in nutritional value (APPENDIX A). However, while the standard mouse diet consists of whole food ingredients including ground corn, wheat middlings, dehulled soybean meal, and ground wheat, the synthetic diet is primarily comprised of single amino acids and synthetically derived vitamins (APPENDIX B and C).

Briefly, methodology for this study: Mouse fecal samples were collected weekly for gut microbiome analysis to monitor modifications to microbial diversity over the course of the feeding period, as well as differential taxa abundance and predicted metabolic pathway alterations at the conclusion of the feeding period. Behavioral tests were then conducted including open-field test, elevated zero maze, and contextual fear conditioning. Mouse colons, blood, and hippocampus tissue were harvested and stored appropriately until further processing. Subsequent analyses of

tissues examine the effects of consuming a synthetic diet on colon length, cytokine levels, and SCFA levels.

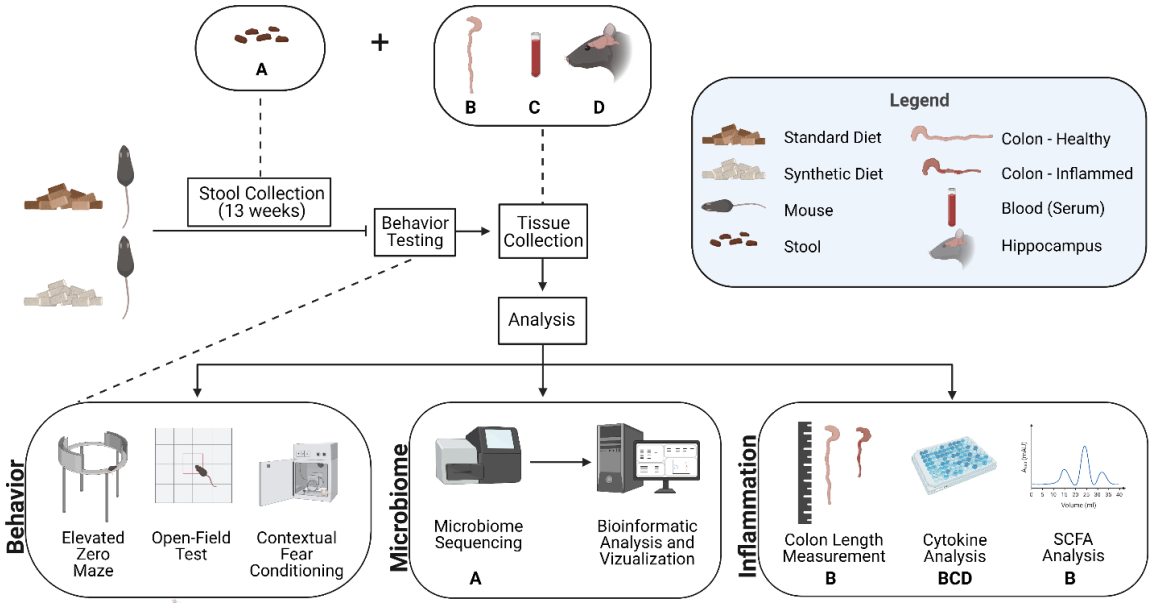

Figure 1. Diagram of experimental design to investigate the effects of consuming a synthetic formula diet on behavior, gut microbiome, and inflammation. Tissue types are denoted by illustrations described in the legend and represented by a letter beneath the assay in which they were examined (A – Stool; B – Colon; C – Blood (serum); D – Hippocampus).

Microbiome

Sample Collection

Mice were briefly separated into individual clean cages with no litter to easily collect fecal pellets on a weekly basis. Samples were collected in individual sterile 1.5ml microcentrifuge tubes and immediately placed over dry ice. After collection, fecal pellets were transferred and stored at -80°C until further processing.

DNA Extraction and 16S rRNA Gene Amplification

DNA was extracted from mouse fecal samples following the manufacturer's protocol for the Kingfisher MagMAX Microbiome Ultra Nucleic Acid Isolation Kit (Thermo Fisher Scientific,

Waltham, Massachusetts). Extracted DNA was eluted to an adjusted final volume of 50µl, quantified using a NanoDrop1000 spectrophotometer (ThermoFisher Scientific Inc., Waltham, MA, USA), and stored at -20°C.

Barcoding polymerase chain reaction (PCR) followed with indexed primers targeting the V4 hypervariable region of the 16S rRNA gene utilizing illumv4_515F (5' – GTGCCAGCMGCCGCGGTAA – 3') and illumv4_806R (5' – GGACTACHVGGGTWTCTAAT – 3') primers with Illumina sequencing adaptors [43]. PCR reactions were prepared in duplicate at 25µl volumes consisting of 2.5 µl 10× Accuprime™ PCR Buffer II (Invitrogen, Carlsbad, CA), 0.5 µl forward and reverse primer (10 µM), 0.1 µl of Accuprime™ Taq DNA Polymerase High Fidelity (5U/µl), 1 µl of template DNA (10-100ng), and 16.9 µl molecular grade water. Negative and positive controls were produced along with every master mix containing either 1-µl *Escherichia coli* genomic DNA or 1 µl of molecular grade water respectively. PCR was carried out as follows: 94°C for 2 minutes, 30 cycles of 94°C for 30 s, 55°C for 40 s, 68°C for 40 s, and a final extension at 68°C for 5 minutes. Successful PCR was confirmed through electroporesis on 1% agarose gels. Bands were observed in all positive PCR controls and absent for all negative controls.

Library Preparation and Sequencing

Duplicate PCR products were pooled and purified using Agencourt® AMPure® XP magnetic beads (Beckman Coulter) following the manufacturer's instruction. Multiplexing was possible through dual indexing using the Nextera XT assay on purified amplicons. Briefly, 50-µl PCR reactions were prepared for each sample with the following recipe and thermocycler protocol: 5 µl 10x Accuprime™ PCR Buffer II, 5 µl Nextera XT Index Primer 1, 5 µl Nextera XT Index Primer 2, 0.2 µl, Accuprime™ Taq DNA Polymerase High Fidelity, 5 µl DNA (~10 pm), and 29.8

µl of molecular grade water; 94°C for 3 minutes, 8 cycles of 94°C for 30 s, 55°C for 30 s, 68°C for 30 s, and a final extension at 68°C for 5 minutes.

Once indexed, PCR products were purified as previously described by AMPure® XP magnetic beads and quantified using the Qubit® 2.0 fluorometer (Invitrogen, Carlsbad, CA). Finally, libraries were pooled at equimolar concentrations then diluted and denatured for a final concentration of 10 pM. Pooled samples were then loaded into the MiSeq Reagent Kit v2 cartridge (Illumina Inc, San Diego, CA) and sequenced on the Illumina MiSeq® instrument, along with an internal control sample consisting of 5% PhiX DNA, for paired-end high-throughput sequencing at 500 cycles.

Controlling for Contamination

In an effort to control for environmental contamination, blanks and negative controls were run alongside samples through the entire process from extraction through sequencing. Blank extractions read below the quantifications limit. Negative controls and blanks amplified in the same 96-well plates as experimental samples did not yield a band in gel elecroporesis. Blank libraries were constructed and also read below quantification limits.

Data Processing

FASTQ files generated by the the Illumina MiSeq® instrument were utilized for bioinformatic processing and microbiome analysis. Sequencing primer reads were trimmed from raw reads using Cutadapt v. 1.16 [76]. Trimmed reads were quality filtered, merged, checked for chimeras, and clustered into Amplicon Sequencing Variants (ASVs) using the DADA2 pipeline [77]. Processed sequences were then assigned taxonomy using VSEARCH v. 2.8.1 and the

EzBiocloud database as a reference. Data analysis was primarily performed within the R version 3.5.0 environment [78, 79].

Microbiome Analysis

Alpha diversity (Shannon diversity index and observed ASV counts) was calculated using phyloseq v. 1.30.0 [80]. Beta diversity was determined through Principal component analysis (PCA) using PhILR transformed data and the Vegan v. 2.5-5 library [81, 82]. Significance of variance found through PCA was determined via permutational multivariate analysis of variance (PERMANOVA) [44].

Differential abundance of ASVs and phylogenetic clades between dietary groups was calculated with DESeq2 and Phylofactor [45, 46]. Additionally, the effect of synthetic diet consumption on the metabolic potential of gut bacteria was predicted through the PICRUSt2 (Phylogenetic Investigation of Communities by Reconstruction of Unobserved States) pipeline [47]. PICRUSt2 results were vizualized with STAMP (STatistical Analysis of Metagenomic Profiles) [83]. The script for all read processing, analyses, and visualization can be accessed at https://github.com/vivmancilla/SyntheticDiet.

Inflammation

Tissue Collection

Following behavioral testing described below, all mice were euthanized via rapid decapitation. Trunk blood was collected and placed on wet ice for 15 minutes, followed by incubation at room temperature for 30 minutes, then centrifugation (2,000 x *g*) at 4° for 10 minutes. Serum was isolated and immediately stored in -80°C until cytokine analysis. Colon tissue and hippocampus from both hemispheres of the brain were extracted. Colons were measured from the

intersection between the cecum and the colon, to the anus. Tissue was lysed, preserved in a protein extraction solution containing protease inhibitors (PRO-PREP, Bulldog Bio, Portsmouth, NH), snap-frozen on dry ice, and stored in -80℃ until processing. Samples were centrifuged (16,820 x *g*) at 4℃ for 20 minutes and finally, clear lysate was extracted and stored at -20℃ until cytokine analysis.

Short Chain Fatty Acid Analysis

Short chain fatty acids (SCFA) in the colon were quantified by Microbiome Insights Inc. (Vancouver, BC, Canada) through gas chromatography (GC) following a similar protocol as in Zhao et al (2006), briefly described here [122]. Colon tissues were resuspended in MilliQ-grade water and homogenized in a MPBio FastPrep for 1 minute at 4.0 m/s. Samples were acidified to a final pH of 2.0 by the addition of 5M HCL. Following acidification, suspensions were incubated and centrifuged at 10,000 RPM to separate the supernatant. Supernatants were spiked with 2-Ethylbutyric acid for a final concentration of 1 mM. Extracted SCFA supernatants were stored in 2-ml GC vials, with glass inserts. SCFA were detected using gas chromatography (Thermo Trace 1310), coupled to a flame ionization detector (Thermo). SCFAs were then detected via direct injection of supernatant into a Thermo TG-WAXMS A GC Column (30 m, 0.32 mm, 0.25 μm). Standard solutions of individual SCFAs were used for calibration.

Cytokine Analysis

Concentrations of proinflammatory cytokines TNFα and IL-6, and anti-inflammatory cytokine IL-10 were quantified in the serum, hippocampal tissue lysates, and colon tissue lysates to assess inflammation using VPLEX Custom Mouse Cytokine Proinflammatory Panel 1 (mouse) multiplexing kits (Meso Scale Diagnostics, Rockville, MD). All wells in the provided plate were

washed three times with a wash buffer before samples were plated. Serum samples were diluted 1:1 in the plates with a proprietary diluent, while hippocampal and colon samples were plated neat. Samples were allowed to incubate at room temperature with shaking horizontally for two hours. All wells were then washed three times with wash buffer, and a detection antibody solution (for TNFα, IL-6, and IL-10 antibodies in 2,820µL of antibody cocktail diluent) was added to each well, followed by a two-hour incubation period at room temperature with shaking. All wells were washed again three more times with a wash buffer. Read buffer was then added to each well, and the electrochemiluminescent signal was read using a QuickPlex SQ 120 instrument (Meso Scale Diagnostics, Rockville, MD). Samples were excluded from analysis if their values fell outside of the standard curve of the assay.

Behavioral Testing

All behavioral testing occurred between 0800 h and 1200 h.

Open Field

We utilized the open field test to measure anxiety-like behavior, exploratory behavior, and locomotor activity in male C57BL/6J mice following 13 weeks of diet consumption. During testing, we utilized four open field maze chambers (27 x 27 cm) and video tracking software (Med Associates Incorporated, St. Albans, VT) to record movement. Prior to behavioral testing, the open field chambers were divided into two separate zones, including the center zone (the center of the chamber) and the outer zone (the remaining space around the center zone). Animals were individually removed from their home cages and placed in the center zone of the open field chamber for 10 minutes, in which they could freely explore. We measured the total duration of

time spent in the center zone (seconds), total vertical counts, the total ambulatory distance traveled (centimeters), and the average speed (centimeters per second).

Elevated Zero

After open field testing, behavior in the elevated zero maze was observed to assess anxiety-like behavior. Mice were placed on an elevated circular platform that is approximately 50 cm tall and 60 cm in diameter. The platform contained alternating quadrants, with two quadrants enclosed with walls and two that were open. Mice were placed individually in an open quadrant, directly facing a closed quadrant, and were allowed to explore the circular platform for a total of five minutes. A camera mounted on the ceiling measured the total distance traveled and total time spent in the open quadrants using EthoVision XT software (Noldus Information Technology, Leesburg, VA). The open quadrants are generally more aversive to mice, so less time spent in the open areas indicates more anxiety-like behavior compared to spending more time in the open areas.

Contextual Fear Conditioning

In the final behavioral test, all mice were trained in a contextual fear conditioning program to investigate the effects of the synthetic diet on cognitive function. In this Pavlovian learning paradigm, mice were placed into an automated chamber containing an electrified grid floor, a polka-dot wall, and a peppermint olfactory cue (Coulbourn Instruments, Whitehall, PA; 17.78 x 17.78 x 30.48 cm) for the training session. After an acclimation period of 120 seconds, mice received a 2-second, mild (0.5mA) footshock. Following the footshock, mice remained in the chamber for an additional 60 seconds before being transported back to their standard home cages. Twenty-four hours following this training session, mice were returned to the conditioning chamber, and freezing behavior was measured for 120 seconds utilizing FreezeFrame™ software

(Actimetrics Software, Wilmette, IL). As freezing is a natural fear response for a mouse, freezing behavior was assessed as the strength of the learned association between the footshock and the conditioning chamber context. In this behavioral paradigm, mice that learn the association between the visual and olfactory context and the aversive footshock exhibit more freezing behavior compared to mice that do not learn this association as well.

Results

Gut Microbiome

Microbiome Diversity Decreased with Consumption of the Synthetic Diet

Changes in diversity of the gut microbiome in the two feeding groups throughout the feeding period were assessed (**Figure 2**). Alpha diversity was determined through calculation of the Shannon diversity index (**Figure 2A**) and by counts of observed number of ASVs for each sampling point (week 0-13) (**Figure 2B**). At weaning (week 0), there was no significant difference in mean Shannon diversity (Synthetic $x = 3.882$, Standard $x = 3.795$, t-test $p = 0.875$). However, by week 13, the synthetic diet group was significantly less diverse (Synthetic $x = 2.485$, Standard $x = 4.595$, t-test $p \leq 0.001$). A similar result was obtained through counts of unique ASVs with no difference found at weaning (Synthetic $x = 205.333$, Standard $x = 202$, t-test $p = 0.959$) and significantly less observed ASVs by week 13 (Synthetic $x = 148.9$, Standard $x = 301.3$, t-test $p \leq 0.001$).

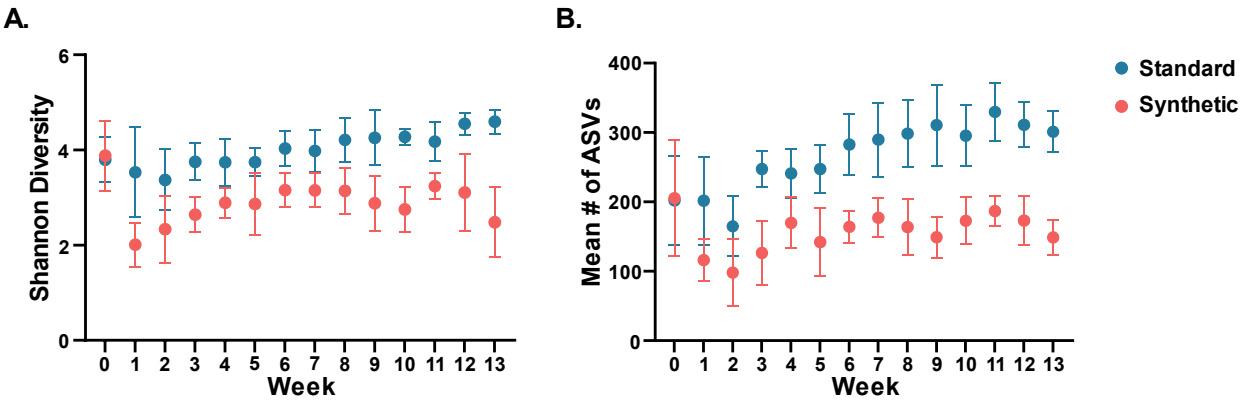

Figure 2. Divergence of gut microbiota alpha diversity (left: number of observed ASVs; right: Shannon diversity index) based on assigned diet plotted from week 0 (weaning) through week 13.

As a measurement of beta diversity, principal component analysis (PCA) of phylogenetic isometric log-ratio (PhILR) transformed distances for the synthetic diet and standard diet animals was conducted for the week 13 dataset (**Figure 3**). PhILR transformed microbiome sequencing data was utilized to produce the PCA plots [81]. At week 13, there is no overlap between samples in the two groups, indicating a dramatic shift of the composition of the gut microbiome caused by the synthetic diet. PERMANOVA determined that the impact of the deviance based on diet (synthetic vs. standard) was statistically significant (R2 = 0.56, p = 0.001), explaining 56% of variance [44].

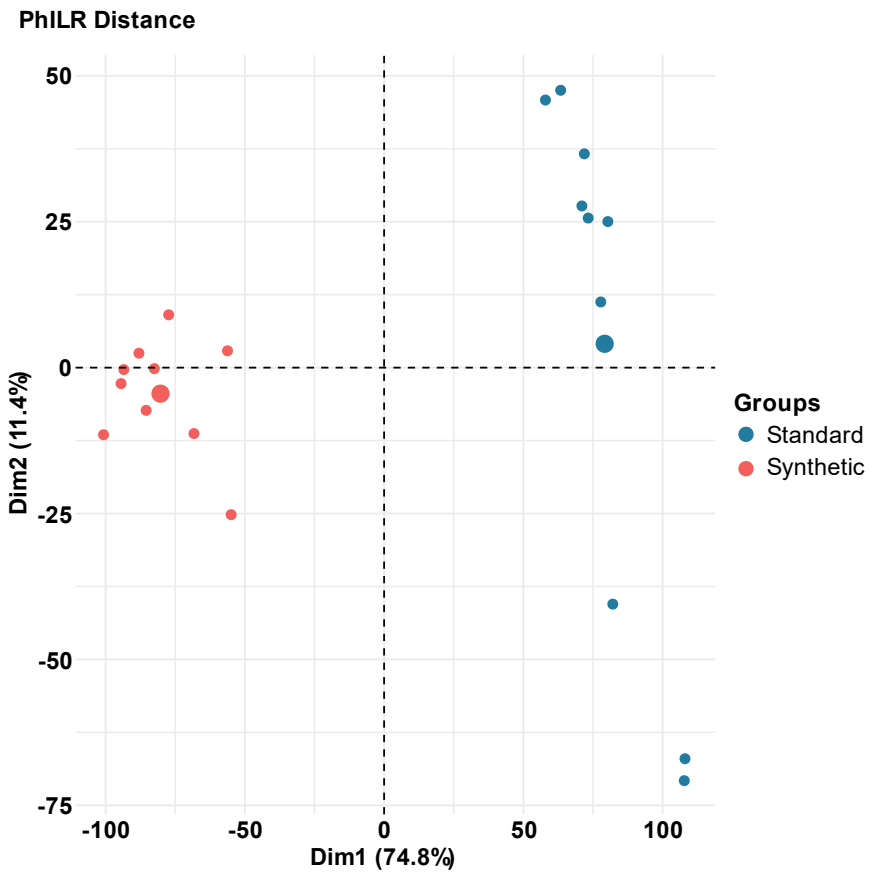

Figure 3. Principal component analysis (PCA) of PhILR distances for the gut microbiota of synthetic and standard diet animals after 13 weeks of feeding on the assigned diet. Individual samples are represented by one point; larger circles represent the mean coordinates for each diet group. (R2 = 0.56, p = 0.001)

Differential Taxa Abundance

DESeq2 identified 76 differentially abundant genera ($p < 0.001$) in the synthetic diet data compared to standard diet data (**Figure 4**). Genera enriched in synthetic diet samples include *Lachnospira*, *Prevotella*, *Lactobacillus*, and *Ruminococcus*. Alternatively, genera that were depleted in the synthetic diet samples include *Faecalibaculum*, *Bacteroides*, *Akkermansia*, and *Oscillibacter*.

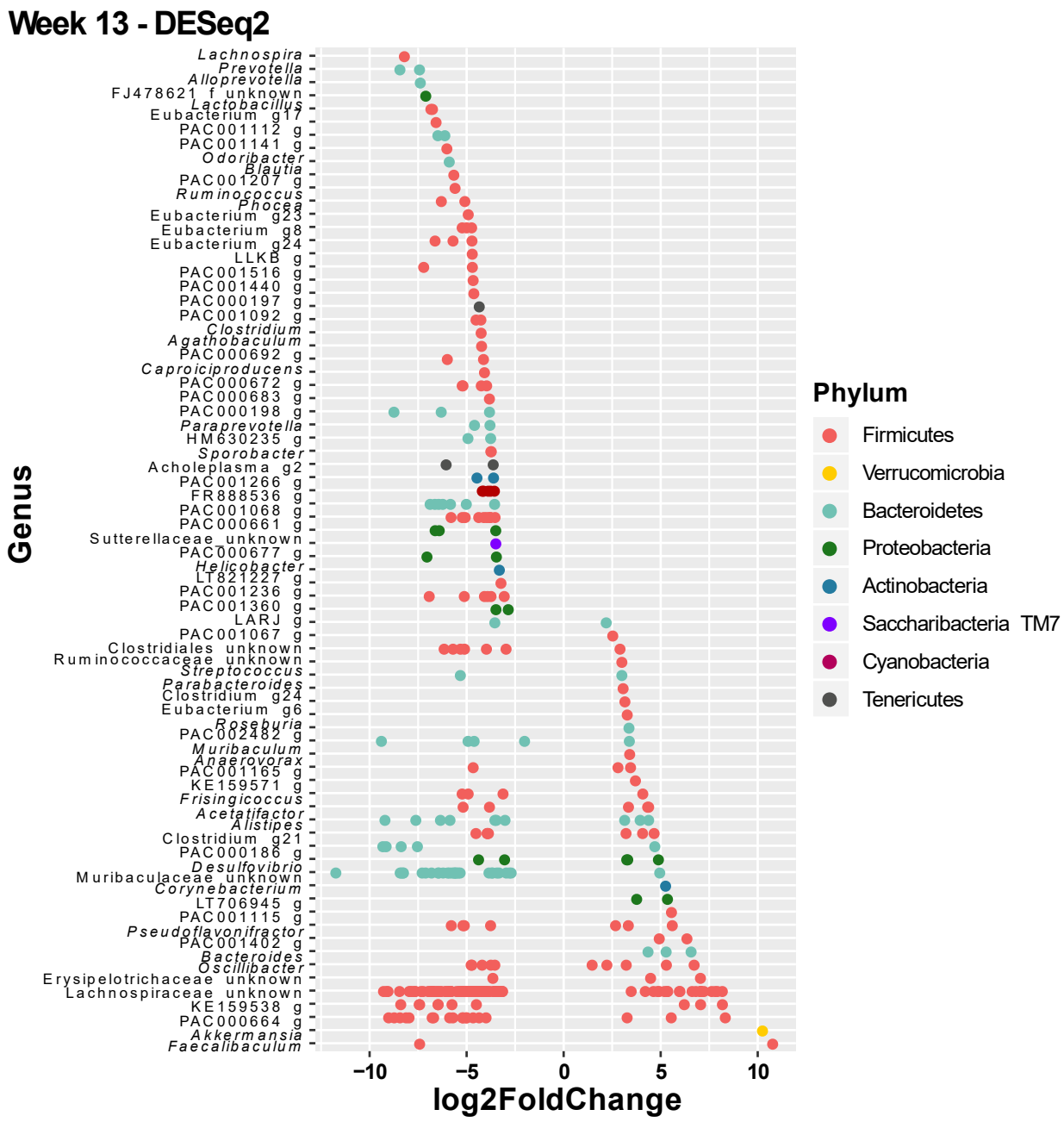

Figure 4. DESeq2 analysis of stool samples collected at week 13 of the feeding period found 76 differentially abundant bacterial genera (y-axis) with in eight phyla (denoted by color). Negative "log2 Fold Change" values (x-axis) indicate higher abundance in synthetic diet animal samples and positive values indicate higher abundances in standard diet animal samples.

In order to identify ASVs which were influential drivers in the variation between the two diet groups at week 13, phylofactor analysis was conducted (**Figure 5**) [46]. Phylofactorization involves all bacterial ASVs present in stool samples from mice fed either a synthetic or standard diet at week 13 (**Figure 5A**). Three factors (family clades) were identified as drivers of variation between the two diet groups: *Erysipelotrichaceae* was enriched in the synthetic diet group (purple; $p < 0.001$) (**Figure 5B**), *Prevotellaceae* was depleted in the synthetic diet group (blue; $p < 0.001$) (**Figure 5C**), and *Muribaculaceae* was depleted in the synthetic diet group (yellow; $p < 0.001$) (**Figure 5D**).

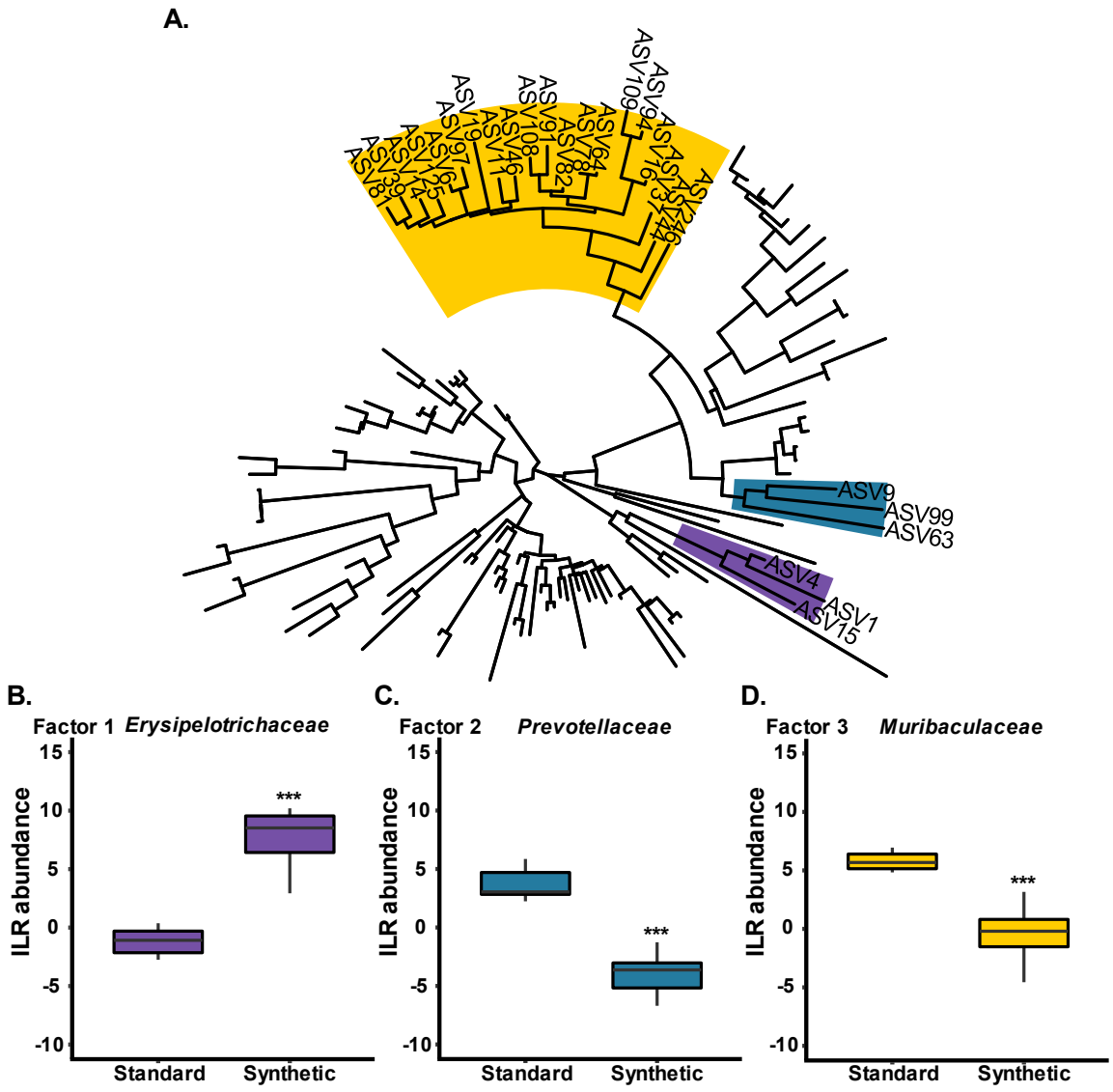

Figure 5. Phylofactorization of all bacterial ASVs present in stool samples from mice fed either a synthetic or standard diet at week 13 (**A**). Three factors (family clades) were identified as drivers of variation between the two diet groups: (**B**) *Erysipelotrichaceae* (purple), (**C**) *Prevotellaceae* (blue), and (**D**) *Muribaculaceae* (yellow). (***$p \leq 0.001$)

Predicted Impact on Gut Bacteria Metabolic Function

Following the characterization of shifts in microbial diversity and the gut microbiome composition associated with the synthetic diet, the next step involved exploring the metabolic pathways that might be affected by these variations. Metabolic predictions were carried out on

microbiome data collected at week 13 of the feeding period using PICRUSt2 (**Figure 6**) [47]. Considering the dramatic deviation in the gut bacterial profile seen in the week 13 PCA (**Figure 3**), 46 pathways were found to be significantly altered in the synthetic diet group compared to the standard group (Welch's inverted method with Bonferroni corrections for multiple comparisons: 46 pathways $p \leq 0.05$) (APPENDIX E). Illustrated in Figure 6 are the top 14 pathways ($p \leq 0.001$). Possible functions affected include fermentation, sulfate reduction, and amino acid biosynthesis.

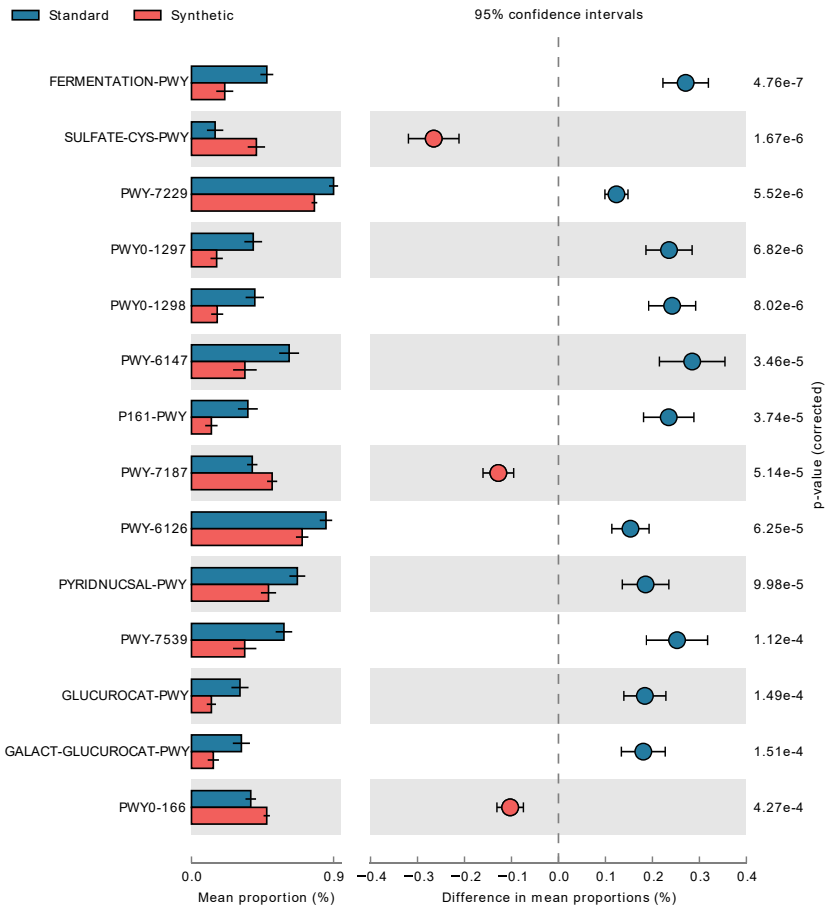

Figure 6. PICRUSt2 analysis predicted 14 metabolic pathways may be affected by the consumption of the synthetic formula diet (coral) compared to the standard diet (blue), based on microbiota present in the gut microbiome in mice in each dietary group at week 13. The colored bars represent 95% confidence intervals calculated using Welch's inverted method ($p \leq 0.05$ with Bonferroni corrections for multiple comparisons. The colored circles represent the difference in mean proportions between synthetic diet and standard diet animal samples.

Inflammation

Colon Length

Colon shortening was used as a marker of inflammation. Decreased colon length has been shown previously in studies on colitis [55, 123, 124]. Despite no difference in body weight (**Figure 7A**), mice fed the synthetic formula diet were found to have significantly shorter colons (cecum to anus). Synthetic diet animals (7.85 cm ± 0.65) had a significantly shorter colon than that of standard diet animals (9.83 cm ± 0.48), $p = 2.65\text{x}10^{-07}$ (**Figure 7B**). Representative photos of colons extracted from mice in the synthetic diet and standard diet group (**Figure 7C**).

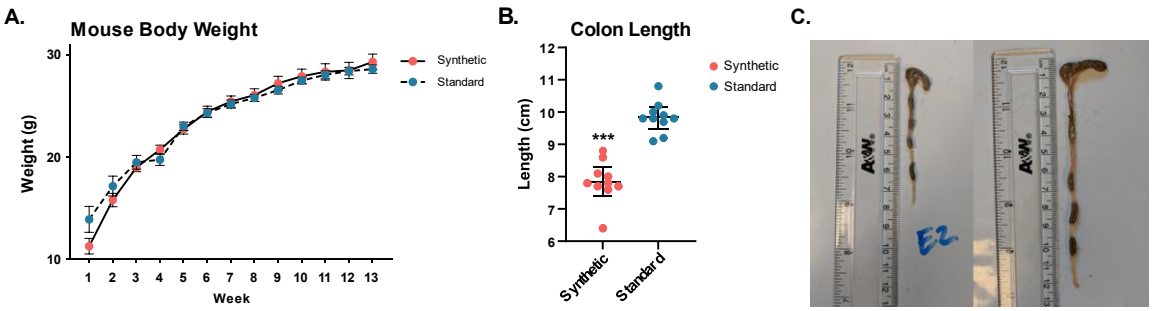

Figure 7. Mouse body weights and colon length measurements of mice fed the synthetic diet or the standard diet after 13 weeks. Body weight for all mice was measured weekly throughout the 13-week feeding period (**A**). Synthetic diet animals (7.85 cm ± 0.65) had a significantly shorter colon than that of standard diet animals (9.83 cm ± 0.48), $p = 2.65\text{x}10^{-07}$ (**B**). Representative photos of colons dissected from synthetic diet animals (**C** – left) and standard diet animals (**C** – right). (***$p \leq 0.001$)

Short Chain Fatty Acid Analysis

Short chain fatty acids are produced as a byproduct of anaerobic fermentation by commensal gut bacteria in the colon. SCFA concentrations were measured in the colon tissue following the 13-week feeding period through gas chromatography and normalized by sample mass (**Figure 8**).

Acetic acid was lower in the synthetic diet group than the standard diet group (7.43 ± 3.17 vs 6.39 ± 8.58, one-tailed *t*-test $p = 0.04$). Propionic acid concentrations were also found to be lower in the synthetic diet animals (2.31 ± 0.96 vs 4.34 ± 2.02, one-tailed *t*-test $p = 0.04$). Butyric acid concentrations were significantly lower in the synthetic diet animal samples (1.09 ± 0.56 vs 4.16 ± 2.04, one-tailed *t*-test $p = 0.01$).

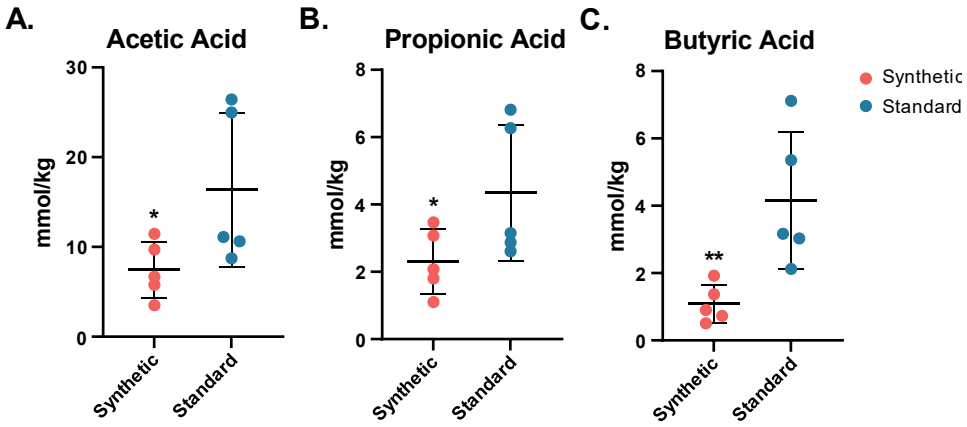

Figure 8. SCFA concentrations (mmol/kg) in colon tissue of mice fed the synthetic diet or the standard diet after 13 weeks. (**A**) Acetic acid synthetic mean (7.43 ± 3.17), standard mean (16.39 ± 8.58), t-test one tail $p = 0.04$; (**B**) Propionic acid synthetic mean (2.31 ± 0.96), standard mean (4.34 ± 2.02), t-test one tail $p = 0.04$; (**C**) Butyric acid synthetic mean (1.09 ± 0.56), standard mean (4.16 ± 2.04), t-test one tail $p = 0.01$. (*$p \leq 0.05$; **$p \leq 0.01$)

Cytokines

Independent samples *t*-tests were performed to investigate the effects of consuming the synthetic diet on proinflammatory cytokines TNFα and IL-6 and anti-inflammatory cytokine IL-10 in the serum, hippocampus, and colon (**Figure 9**). In the serum IL-6 analysis, homogeneity of variance was violated. Thus, two samples that were determined to be outliers by SPSS's interquartile range rule were excluded from analysis. Results revealed a significant difference in serum IL-6 ($t(9) = 2.408$, $p = 0.020$) and in serum TNFα ($t(9) = 2.292$, $p = 0.024$) such that the synthetic diet mice had higher serum levels of IL-6 and lower in TNFα compared to control diet mice. Results revealed no significant difference in serum IL-10 ($t(9) = -0.721$, $p = 0.245$).

By contrast, colon tissue analyses revealed no significant differences in levels of IL-6 ($t(4) = 0.836$, $p = 0.225$) or TNFα ($t(4) = -1.381$, $p = 0.120$)) between synthetic diet mice and standard control diet mice. However, colon IL-10 ($t(2) = -81.53$, $p = 0.008$) was significantly lower in mice fed the synthetic diet.

Results from the brain revealed that levels of TNFα ($t(9) = 2.074$, $p = 0.034$) and IL-6 ($t(9) = 5.722$, $p < 0.001$) were significantly higher in the hippocampus of mice fed a synthetic diet compared to standard control diet mice. Hippocampal IL-10 was unable to be assessed, as values from all synthetic diet mice and all but four standard diet mice fell below the standard curve of the assay.

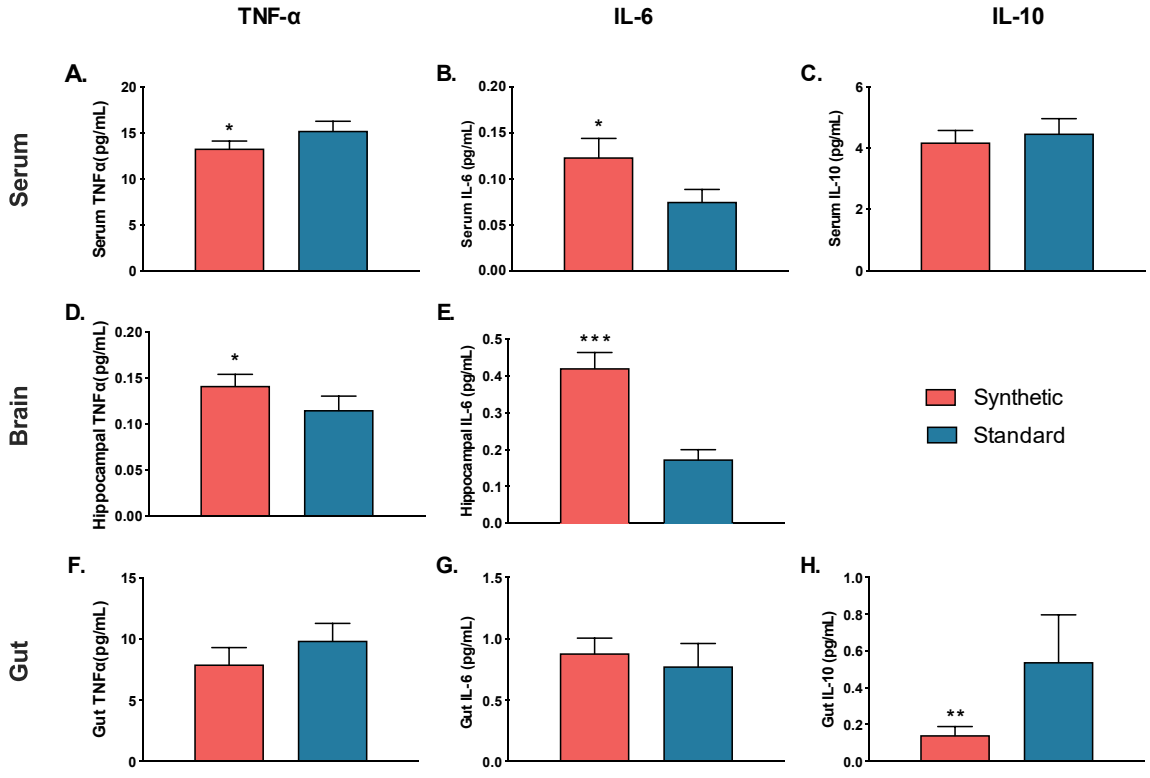

Figure 9. Cytokine (TNF-α, IL-6, IL-10) quantification in the serum, hippocampus tissue lysate (brain), and colon tissue lysate (gut). (**A**) Serum TNF-α*; (**B**) Serum IL-6*; (**C**) Serum IL-10; (**D**) Hippocampal TNF-α*; (**E**) Hippocampal IL-6***; (**F**) Gut TNF-α; (**G**) Gut IL-6; (**H**) Gut IL-10**. Hippocampal IL-10 was excluded. *$p \leq 0.05$; **$p \leq 0.01$; ***$p \leq 0.001$

Behavior

Open Field Test

Independent samples *t*-tests were performed to analyze the effects of the synthetic diet on anxiety-like behavior, exploratory behavior, and locomotor activity in the open field test (**Figure 10**). The results revealed no significant differences between the total time spent in the center zone ($t(18) = 1.46$, $p = 0.16$), or the total vertical counts, ($t(18) = 0.96$, $p = 0.35$). However, the results revealed a difference in the total distance traveled (cm) that was approaching significance ($t(18) = 1.85$, $p = 0.08$), such that mice on the synthetic diet traveled moderately farther than those on the standard control diet. Additionally, results revealed a significant difference between the total average speed, ($t(17) = 2.33$, $p = 0.03$), such that mice on the synthetic diet traveled significantly faster than mice on the standard control diet.

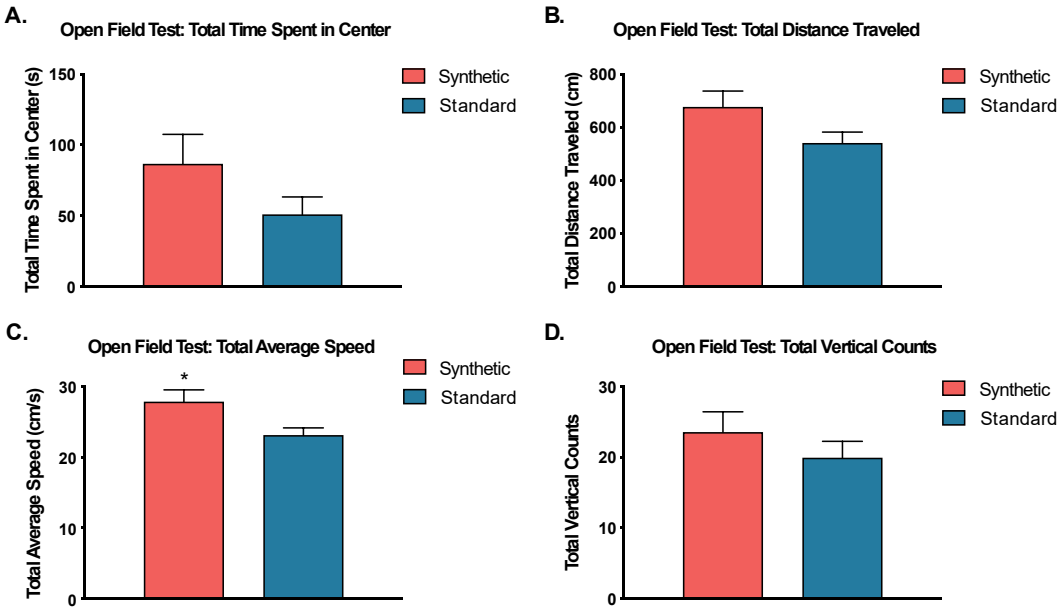

Figure 10. Open Field Test. An independent samples *t*-test was used to compare behavior in the open field chamber between animals fed synthetic diet (coral) and a standard diet (blue) for (**A**) total time spent in the center zone, (**B**) total distance traveled, (**C**) total average speed, and (**D**) total vertical counts. While all cases revealed higher average values for synthetic diet fed mice, only total average speed (C) was significantly different (*$p \leq 0.05$).

Elevated Zero Maze

Independent samples *t*-tests were performed to analyze the effects of the synthetic diet on motor and anxiety-like behaviors in the elevated zero maze (**Figure 11**). Results revealed no significant differences between time in open quadrants ($t(18) = 1.52$, $p = 0.15$), latency to first entry of an open quadrant ($t(18) = 0.08$, $p = 0.94$), number of entries to the open quadrants ($t(18) = 0.90$, $p = 0.38$), total distance traveled ($t(18) = 1.01$, $p = 0.29$), or velocity ($t(18) = 0.96$, $p = 0.35$) between mice that consumed the synthetic diet versus mice that consumed the standard control diet, although in all cases values were slightly higher for mice on the synthetic diet.

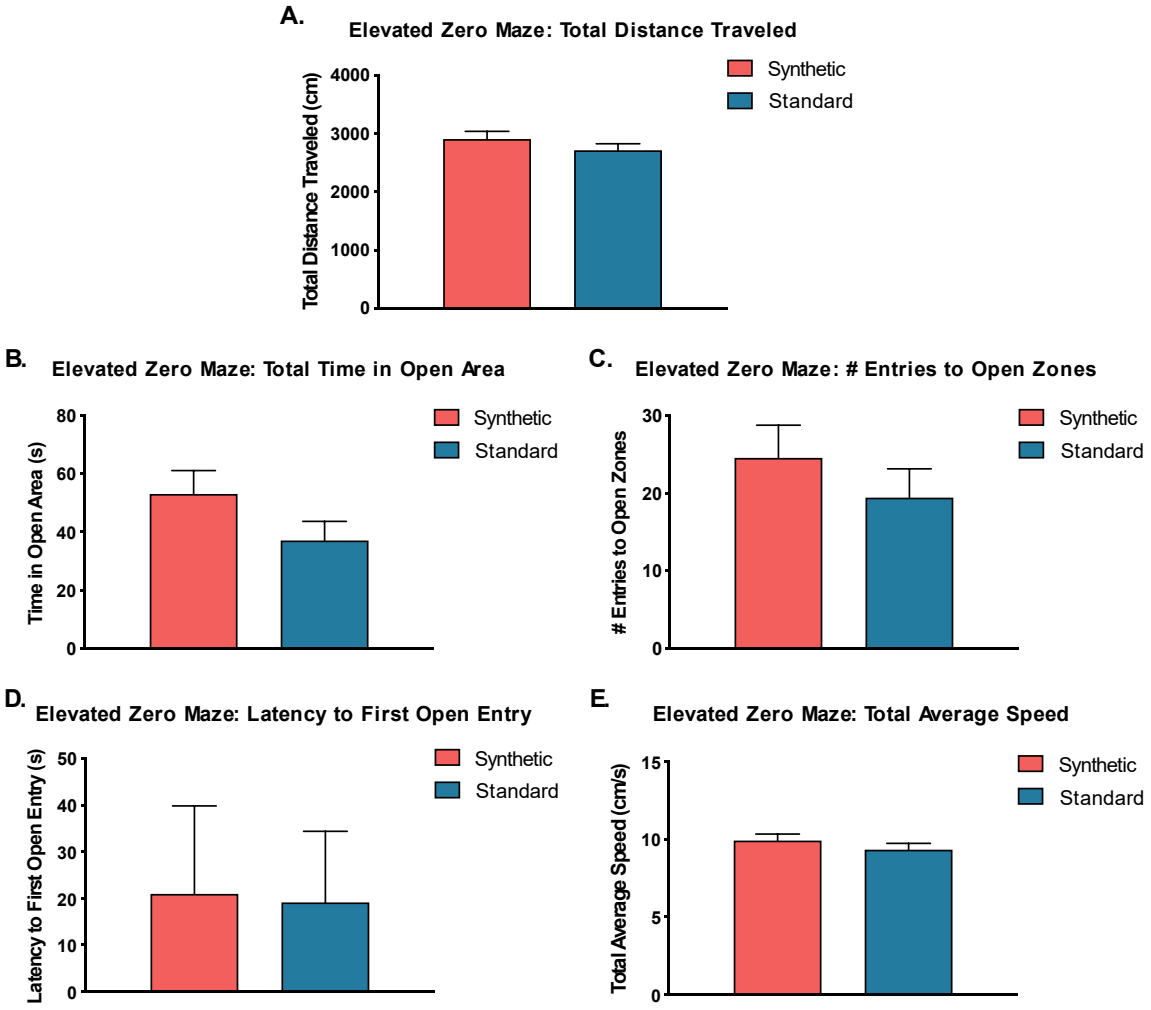

Figure 11. Elevated Zero Maze. (**A**) Total distance traveled in synthetic and standard diet animals; (**B**) Total time in open areas; (**C**) Number of entries into the open areas or zones; (**D**) Latency to first entry into an open zone; (**E**) Total average speed. No significant differences were detected by independent samples *t*-tests.

Contextual Fear Conditioning

An independent samples *t*-test was also performed to assess the effects of the synthetic diet on cognitive function (**Figure 12**). Results revealed no significant difference in freezing behavior between mice fed the synthetic diet and mice fed the standard control diet ($t(18) = -0.26$, $p = .81$).

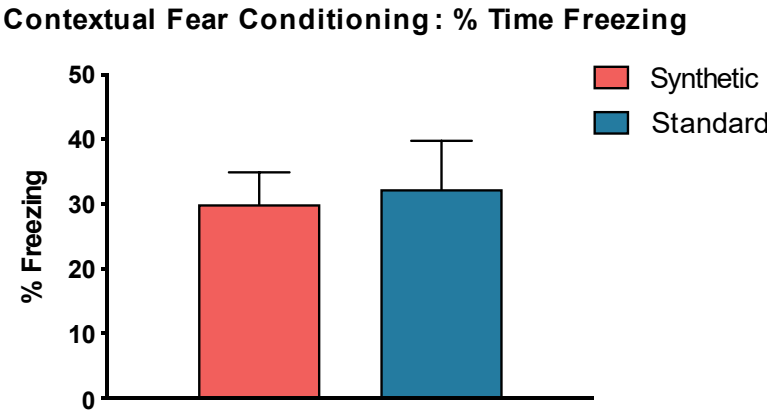

Figure 12. Contextual Fear Conditioning. An independent samples *t*-test revealed no significant difference in percent freezing time between synthetic and standard diet animal following a footshock training day ($t(18) = -0.26$, $p = 0.80$, $n = 10$).

Discussion

The gut microbiome has been implicated in health and disease through the roles that resident bacteria play in nutritional absorption, metabolite production, education of the immune system, and interactions with distal organs (i.e., the gut-brain axis). Additionally, decreased gut microbiome diversity has been associated with a variety of disease states [14]. Diet is frequently reported as major driving force microbiome composition. Here, we assessed the effects of a largely synthetic diet analogous to those typically prescribed for PKU patients and others with genetic inborn errors of amino acid metabolism. Wild type mice were chosen for this study, rather than a metabolism disorder mouse model in order to isolate the synthetic formula diet as a factor in the modulation of the gut microbiome previously seen in metabolic disorders such as PKU [48, 49, 125]. In a review by Colonetti, et al., the importance of studying the interplay between the microbiome and inborn errors of metabolism is discussed [126].

Western societies consume higher amounts of processed food while more traditional societies consume more fiber, exhibit have gut higher diversity, and have been shown to contain gut commensal bacteria that are no longer seen in the industrialized societies [40, 52, 95]. Western diets typically contain less microbially accessible carbohydrates (MACs), possibly leading to the starving out of bacterial groups [40, 114]. Gut microbial diversity has been noted as protective by contributing to stability and resilience against major changes, and higher diversity is also associated with higher genetic and enzyme diversity [38, 115, 127]. In mice consuming an oversimplified and highly processed synthetic diet, we detected a drop in Shannon diversity index and ASV counts after the first week that continued and strengthened throughout the 13-week course of the study, such that these diversity measures for synthetic-diet fed mice were ultimately lower than their initial post-weaning baseline.

Comparative taxa abundance showed an increased presence of bacteria previously associated with disease and inflammation. For example, *Prevotella* was significantly more abundant in the mice fed the synthetic diet. In a recent study, investigators reported that mice colonized with certain *Prevotella* sp. exhibited several markers of inflammation including shortening of the colon, increased pro-inflammatory IL-6 in the gut and decreased anti-inflammatory IL-10, similar to that reported here for mice in the synthetic diet group [128].

A representative PCA plot of the synthetic diet and standard diet microbiome data illustrate the drama shift of the microbiome over the course of the feeding period (**Figure 3**). This shift can be seen based on the distances between data points representative of each feeding group and verified through PERMANOVA [44]. Our results indicated that the difference between the microbiome data of the two diet groups was statistically significant and 56% of the variance could be explained by the diet group assignments.

Metabolic predictions are predicted by combining the microbiome data with open sources of known bacterial pathways (**Figure 6**). Our results demonstrated several pathways were affect by a 13-week period, beginning at weaning, of feeding on the synthetic diet instead of the standard diet. Many of the pathways highlighted through the predictions contribute to fermentation, as well as sulfate reduction and amino acid biosynthesis. The colon is the site for the anaerobic fermentation of indigestible dietary fibers which provide SCFAs including acetate, propionate, and butyrate [15]. SSCFAs have been shown to be protective against colitis and general inflammation in the gut by decreasing the colonic pH, neutralizing toxins, and preventing the adhesion of pathogenic microbes in the gut [16-20]

A dramatic decrease in colon length was found at the time of tissue collection in this study. Colon measurements are an accepted indicator of inflammation and colitis [55, 123, 128, 129]. This shortening of the colon has possible implications with nutritional absorption and could be, in part, caused by the inability for nutritionally depleted colonocytes to enter a maintenance phase. In this study, significantly lower SCFA levels were also found in the colon of the synthetic diet mice. Butyrate is known to be a major energy source for colonocytes and is produced as a byproduct of the fermentation of soluble fibers by resident colonic bacteria [15, 24, 130]. Therefore, the consumption of dietary fibers is believed to result in increased production of SCFAs, allowing colonocytes to enter maintenance phase, supporting the structure of tight junctions and enhancing the gut barrier [56, 57, 102, 131]. Multiple studies have shown improvement of symptoms in several diseases and disorders with the addition of SCFAs or dietary fiber [21, 52, 86, 87, 117, 129, 130, 132].

In addition to dysbiosis and elevated markers of inflammation, the mice on the synthetic diet exhibited modified behavior. Mice as prey animals will typically avoid open areas,

maintaining their bodies close to walls or cover. These types of fear behaviors are widely accepted as models of anxiety of anxiolytic behavior [133]. Interestingly, mice on the synthetic diet in this study exhibited significantly higher average speeds in the open field test, and tended to spend more time in the open, suggesting a possibly reduced fear response. Additionally, changes in cognition were observed through contextual fear conditioning. Mice on the synthetic diet displayed abnormal behavior as they were shown to travel more and faster, spending more time in open areas, and generally exhibiting more exploratory behavior. The synthetic diet mice also spent less time freezing during the testing day of contextual fear conditioning, while no difference was shown in freezing times during the training day. The results indicate that mice on the standard diet were able to learn the association between the CFC box and a footshock, while the synthetic animals did not.

In conclusion, we demonstrated that the consumption of a synthetic diet led to the emergence of indicators of dysbiosis in the gut microbiota, markers of inflammation, and the evolutionarily inappropriate behavior in wild type mice. The synthetic diet tested here was not high fat as compared with what is known as the "Western diet". However, mice on the synthetic diet showed multiple markers of inflammation and concomitant losses of bacteria thought to be anti-inflammatory, similar to that reported for studies of the Western diet [5, 52]. The results suggest that the reported effects of the Western diet may be more strongly influenced by the lack of microbially accessible fiber rather than to increased fat or meat intake. The findings also have implications for the application of such restricted diets as medical interventions in patients with PKU or other genetic inborn errors of metabolism. While more research is necessary to tease out the individual effects of replacement of complex proteins with amino acids versus decreases in complex carbohydrates, the data suggest that such diets should also consider microbially accessible carbohydrate fibers as necessary components.

CHAPTER IV

CONCLUSION

The first of the enclosed studies investigated the effect of the PKU treatment on the composition, diversity, and metabolic function of the gut microbiome in adults diagnosed with PKU. 16S rRNA gene sequencing of fecal samples from PKU and non-PKU adults demonstrated a reduction of alpha diversity in PKU samples, although the measurements were not statistically significant. These findings were surprising considering previous studies of PKU children found they had significantly lower gut microbiota diversity. We then characterized the composition of the adult PKU gut microbiome. This was the first time that the gut microbiome of PKU adults has been described through 16S rRNA sequencing.

Further investigation is necessary to determine if the PKU diet and treatment has a more pronounced impact on the gut microbiome of children, which is still developing and not as stable as the adult gut microbiome [95, 134]. Alternatively, differences in microbial diversity between PKU children and adults may be a function of a more regulated diet in children, as, typically, parents are planning meals and maintaining a sense of stability, which may lead to better adherence to the diet and subsequently a more dramatic drop in gut microbial diversity. Adults with PKU, on the other hand, may deviate more often from the prescribed diet [59, 62, 135]. Consistent with that hypothesis, and self-reported dietary consumption by participants revealed a high level of variability in dietary adherence among patients. Additionally, routine neonatal

screenings and immediate prescription for treatment are recent advancements seen within the last 50 years for PKU [136].

PKU samples contained lower relative abundance of anti-inflammatory microbes, including the genera, *Faecalibacterium*. *Faecalibacterium* sp. are known to be one of the most abundant taxa in the healthy human gut microbiome [137, 138]. They are major producers of butyrate, an energy source for colonocytes, through fermentation of soluble fibers in the large intestine [85, 139]; they are also the only known producers of Microbial Anti-Inflammatory Molecule (MAM), a protein compiled of peptides capable of inhibiting the NF-κB pathway [140, 141]. Low levels of *F. prausnitzii* have also been implicated in disorders associated with dysbiosis [27, 89, 142].

Finally, metabolic function predictions revealed the potential enrichment of pathways involved in carbon fixation and carbohydrate fermentation. Interestingly, the N-acetylneuraminate degradation pathway was increased, which is has also been shown in immunocompromised individuals to aid in the proliferation of pathogenic bacteria and permeation into the bloodstream [99].

Additional information was collected from study participants through self-reported questionnaires, although the included study focused on the diagnosis of PKU as the primary factor. Future directions may include expanding the sample size to account for additional variable factors such as treatment type (i.e., diet, sapropterin dihydrochloride administration, enzyme replacement therapy), dietary adherence, and severity of PKU.

In the murine synthetic diet study, we demonstrated that consumption of a synthetic amino acid diet quickly led to dysbiosis of the gut microbiome, elevated markers of inflammation, and evolutionarily inappropriate behavior in wild-type mice.

We were able to show that the diet can cause a shift in the gut microbiome and a reduction of diversity after only one week of consumption. Decreased diversity of a community typically indicates underlying dysbiosis due to accompanying instability and reduction of resilience [38]. Metabolic potential for pathways involving fermentation, sulfate reduction, amino acid biosynthesis, and others were also affected by the variance in taxa abundance. Inflammation was determined by shrinkage of the colon, decreased SCFA quantifications, and altered cytokine levels in various tissue types (serum, hippocampus, colon). Many of these diet-driven effects we demonstrated were dramatic and followed our initial expectations.

Initially, we expected to see increased indicators of anxiety in the synthetic diet mice due to diet induced dysbiosis and inflammation. Instead, we found that mice on the synthetic diet exhibited significantly higher average speed in the elevated zero maze and open field chamber than the animals on the standard diet. They also spent more time in the open areas during both tests, suggesting a possibly reduced fear response. In contextual fear conditioning, mice are presented with a foreign environment followed by an adverse stimulus, a footshock in this study (training day). Mice are expected to learn the association between the environment and the stimulus, resulting in increased time spent freezing during a reintroduction to said environment in anticipation of the stimulus (testing day). Testing day data revealed that mice on the synthetic diet did spend less time freezing, indicating affected cognition, although the values were not significantly different.

Future studies may aim to validate the causal role of the synthetic diet in the effects seen in synthetic diet mouse group. This could be inferred by the amelioration of the effects by the supplementation of prebiotics, or soluble fiber, to the synthetic diet.

In these studies, we described the gut microbiome of adults with Phenylketonuria for the first time. Many of the comorbidities of PKU have been associated with dysbiosis in the gut. We were able to show that the synthetic nature of the amino acid diet in mice was not supportive of beneficial gut bacteria. Additionally, mice fed a synthetic diet had elevated markers of inflammation and displayed inappropriate behavior when exposed to aversive situations. Presumably, the diet also indirectly affected immune response through weakening of the gut barrier due to depleted production of SCFAs and lack of a nutritional support for anti-inflammatory bacteria; however, these effects were not investigated. These findings demonstrate the importance of a multidisciplinary approach when considering diet and the gut microbiome in diseases and disorders. Lastly, future studies should consider the ecological relationships between microbial groups as well as with the host.

APPENDIX

APPENDIX A. Nutrient Information

	Standard % by weight	**Synthetic** % by weight
Protein	18.2	18.2
CHO	55.8	60.3
Fat	5.2	5.2
Crude Fiber	4.9	5%
kcal/g	3.43	3.6

APPENDIX B. List of Ingredients in Standard Diet

Standard Diet Ingredients:
Ground Corn
Wheat Middlings
Dehulled Soybean Meal
Ground Wheat
Fish Meal
Porcine Animal Fat Preserved with BHA and Citric Acid
Dehydrated Alfalfa Meal
Cane Molasses
Ground Oats
Wheat Germ
Calcium Carbonate
Brewers dried Yeast
Salt
Dried Beet Pulp
Corn Gluten Meal
Ground Soy-Bean Hulls
Soybean Oil
Dried Whey
Porcine Meat and Bone Meal
Dicalcium Phosphate
L-Lysine
Sucrose
DL-Methionine
Menadione Dimethylpyrimidinol Bisulfite
Magnesium Oxide
Vitamin A Acetate
Cholecalciferol
Biotin
DL-Alpha Tocopheryl Acetate
Riboflavin Supplement
Folic Acid
Vitamin B-12 Supplement
Nicotinic Acid
Calcium Pantothenate
Pyridoxine Hydrochloride
Manganous Oxide
Zinc Oxide
Ferrous Carbonate
Copper Sulfate
Zinc Sulfate
Calcium Iodate

Cobalt Carbonate
Sodium Selenite

APPENDIX C. List of Ingredients in Synthetic Diet

Synthetic Diet Ingredients:
L-Alanine
L-Arginine HCl
L-Asparagine
L-Aspartic Acid
L-Cystine
L-Glutamic Acid
L-Glutamine
Glycine
L-Histidine HCl, monohydrate
L-Isoleucine
L-Leucine
L-Lysine HCl
L-Methionine
L-Phenylalanine
L-Proline
L-Serine
L-Threonine
L-Tryptophan
L-Tyrosine
L-Valine
Taurine
Sucrose
Corn Starch
Maltodextrin
Lard
Soybean Oil
Cellulose
Mineral Mix, AIN-93M-MX (94049)
Calcium Phosphate, monobasic, monohydrate
Vitamin Mix, AIN-93-VX (94047)
Choline Bitartrate
TBHQ, antioxidant

APPENDIX D. Fiber Content in Experimental Diets

Diet Condition	% Insoluble Fiber	% Soluble Fiber
Synthetic Diet	5%	0%
Standard Control Diet	8.58%	1.2%

APPENDIX E. PICRUSt2 Results Comparing Data Collected from Mice Fed a Synthetic Diet or the Standard Diet after 13 Weeks post-weaning, $p \leq 0.05$.

Pathway	p-value	In synthetic vs standard	MetaCyc Pathway
FERMENTATION-PWY	4.76E-07	lower	mixed acid fermentation
SULFATE-CYS-PWY	1.67E-06	higher	superpathway of sulfate assimilation and cysteine biosynthesis
PWY-7229	5.52E-06	lower	superpathway of adenosine nucleotides de novo biosynthesis I
PWY0-1297	6.82E-06	lower	superpathway of purine deoxyribonucleosides degradation
PWY0-1298	8.02E-06	lower	superpathway of pyrimidine deoxyribonucleosides degradation
PWY-6147	3.46E-05	lower	6-hydroxymethyl-dihydropterin diphosphate biosynthesis I
P161-PWY	3.74E-05	lower	acetylene degradation (anaerobic)
PWY-7187	5.14E-05	higher	pyrimidine deoxyribonucleotides de novo biosynthesis II
PWY-6126	6.25E-05	lower	superpathway of adenosine nucleotides de novo biosynthesis II
PYRIDNUCSAL-PWY	9.98E-05	lower	NAD salvage pathway I (PNC VI cycle)
PWY-7539	1.12E-04	lower	6-hydroxymethyl-dihydropterin diphosphate biosynthesis III (Chlamydia)

GLUCUROCAT-PWY	1.49E-04	lower	superpathway of β-D-glucuronosides degradation
GALACT-GLUCUROCAT-PWY	1.51E-04	lower	superpathway of hexuronide and hexuronate degradation
PWY0-166	4.27E-04	higher	superpathway of pyrimidine deoxyribonucleotides de novo biosynthesis (E. coli)
GLYOXYLATE-BYPASS	1.32E-03	higher	glyoxylate cycle
PWY-5659	1.41E-03	higher	GDP-mannose biosynthesis
PWY-6385	1.56E-03	lower	peptidoglycan biosynthesis III (mycobacteria)
SO4ASSIM-PWY	2.00E-03	higher	assimilatory sulfate reduction I
PWY-7199	2.12E-03	lower	pyrimidine deoxyribonucleosides salvage
PWY-7197	4.07E-03	higher	pyrimidine deoxyribonucleotide phosphorylation
PWY-7222	5.33E-03	lower	guanosine deoxyribonucleotides de novo biosynthesis II
PWY-7220	5.33E-03	lower	adenosine deoxyribonucleotides de novo biosynthesis II
BIOTIN-BIOSYNTHESIS-PWY	7.11E-03	higher	biotin biosynthesis I
PWY-5971	9.65E-03	higher	palmitate biosynthesis (type II fatty acid synthase)
PWY-5667	0.01	lower	CDP-diacylglycerol biosynthesis I
PWY0-1319	0.01	lower	CDP-diacylglycerol biosynthesis II
PWY0-1586	0.01	lower	peptidoglycan maturation (meso-diaminopimelate containing)
PWY-7392	0.011	higher	taxadiene biosynthesis (engineered)
PWY-7664	0.012	higher	oleate biosynthesis IV (anaerobic)
PWYG-321	0.012	higher	mycolate biosynthesis
PWY-6891	0.013	higher	thiazole component of thiamine diphosphate biosynthesis II
PWY0-862	0.014	higher	(5Z)-dodecenoate biosynthesis I
PWY-6282	0.015	higher	palmitoleate biosynthesis I (from (5Z)-dodec-5-enoate)
PWY-6519	0.015	higher	8-amino-7-oxononanoate biosynthesis I

PWY-5484	0.016	higher	glycolysis II (from fructose 6-phosphate)
PWY-5989	0.017	higher	stearate biosynthesis II (bacteria and plants)
FASYN-INITIAL-PWY	0.018	higher	superpathway of fatty acid biosynthesis initiation (E. coli)
GALACTUROCAT-PWY	0.021	lower	D-galacturonate degradation I
P441-PWY	0.022	lower	superpathway of N-acetylneuraminate degradation
PWY-2942	0.025	lower	L-lysine biosynthesis III
PWY-7456	0.034	higher	β-(1,4)-mannan degradation
POLYAMINSYN3-PWY	0.034	lower	superpathway of polyamine biosynthesis II
HEMESYN2-PWY	0.035	lower	heme b biosynthesis II (oxygen-independent)
PWY-6353	0.042	lower	purine nucleotides degradation II (aerobic)
PWY-7184	0.046	higher	pyrimidine deoxyribonucleotides de novo biosynthesis I
ARG+POLYAMINE-SYN	0.048	lower	superpathway of arginine and polyamine biosynthesis

REFERENCES

1. Williams, R.A., C.D. Mamotte, and J.R. Burnett, *Phenylketonuria: an inborn error of phenylalanine metabolism.* Clin Biochem Rev, 2008. **29**(1): p. 31-41.
2. Al Hafid, N. and J. Christodoulou, *Phenylketonuria: a review of current and future treatments.* Transl Pediatr, 2015. **4**(4): p. 304-17.
3. Hoeks, M.P., M. den Heijer, and M.C. Janssen, *Adult issues in phenylketonuria.* Neth J Med, 2009. **67**(1): p. 2-7.
4. Louis, P., et al., *Understanding the effects of diet on bacterial metabolism in the large intestine.* J Appl Microbiol, 2007. **102**(5): p. 1197-208.
5. Turnbaugh, P.J., et al., *The effect of diet on the human gut microbiome: a metagenomic analysis in humanized gnotobiotic mice.* Sci Transl Med, 2009. **1**(6): p. 6ra14.
6. Wu, G.D., et al., *Linking long term dietary patterns with gut microbial enterotypes.* Science Mag, 2011.
7. Langdon, A., N. Crook, and G. Dantas, *The effects of antibiotics on the microbiome throughout development and alternative approaches for therapeutic modulation.* Genome Medicine, 2016. **8**: p. 39.
8. Khachatryan, Z.A., et al., *Predominant role of host genetics in controlling the composition of gut microbiota.* PLoS One, 2008. **3**(8): p. e3064.
9. Dave, M., et al., *The human gut microbiome: current knowledge, challenges, and future directions.* Transl Res, 2012. **160**(4): p. 246-57.
10. Xu, J. and J.I. Gordon, *Honor thy symbionts.pdf.* PNAS, 2003. **100**(18): p. 10452–10459.
11. Neufeld, K.M., et al., *Reduced anxiety-like behavior and central neurochemical change in germ-free mice.* Neurogastroenterol Motil, 2011. **23**(3): p. 255-64, e119.
12. Stilling, R.M., et al., *Friends with social benefits: host-microbe interactions as a driver of brain evolution and development?* Front Cell Infect Microbiol, 2014. **4**: p. 147.
13. Berbers, R.M., et al., *Microbial Dysbiosis in Common Variable Immune Deficiencies: Evidence, Causes, and Consequences.* Trends Immunol, 2017. **38**(3): p. 206-216.
14. Carding, S., et al., *Dysbiosis of the gut microbiota in disease.* Microb Ecol Health Dis, 2015. **26**: p. 26191.
15. den Besten, G., et al., *The role of short-chain fatty acids in the interplay between diet, gut microbiota, and host energy metabolism.* J Lipid Res, 2013. **54**(9): p. 2325-40.
16. Vieira, A.T., M.M. Teixeira, and F.S. Martins, *The role of probiotics and prebiotics in inducing gut immunity.* Front Immunol, 2013. **4**: p. 445.
17. Scheppach, W., *Effects of short chain fatty acids on gut morphology and function.* Gut, 1994. **35**(1 Suppl): p. S35-S38.
18. Miquel, S., et al., *Identification of metabolic signatures linked to anti-inflammatory effects of Faecalibacterium prausnitzii.* MBio, 2015. **6**(2).
19. Meijer, K., P. De Vos, and M.G. Priebe, *Butyrate and other short-chain fatty acids as modulators of immunity: What relevance for health?* Current Opinion in Clinical Nutrition and Metabolic Care, 2010. **13**(6): p. 715-721.
20. Kawasaki, Y., et al., *Inhibition by lactoferrin and kappa-casein glycomacropeptide of binding of Cholera toxin to its receptor.* Biosci Biotechnol Biochem, 1992. **56**(2): p. 195-8.
21. Smith, P.M., et al., *The Microbial Metabolites, Short-Chain Fatty Acids, Regulate Colonic T_{reg} Cell Homeostasis.* Science, 2013. **341**(6145): p. 569-573.
22. Park, J., et al., *Short-chain fatty acids induce both effector and regulatory T cells by suppression of histone deacetylases and regulation of the mTOR-S6K pathway.* Mucosal Immunol, 2015. **8**(1): p. 80-93.
23. Roediger, W.E., *Role of anaerobic bacteria in the metabolic welfare of the colonic mucosa in man.* Gut, 1980. **21**(9): p. 793-8.

24. Macfarlane, G.T. and S. Macfarlane, *Fermentation in the human large intestine: its physiologic consequences and the potential contribution of prebiotics.* J Clin Gastroenterol, 2011. **45 Suppl**: p. S120-7.
25. Sonnenburg, Erica D. and Justin L. Sonnenburg, *Starving our Microbial Self: The Deleterious Consequences of a Diet Deficient in Microbiota-Accessible Carbohydrates.* Cell Metabolism, 2014. **20**(5): p. 779-786.
26. Wang, W., et al., *Increased proportions of Bifidobacterium and the Lactobacillus group and loss of butyrate-producing bacteria in inflammatory bowel disease.* J Clin Microbiol, 2014. **52**(2): p. 398-406.
27. Machiels, K., et al., *A decrease of the butyrate-producing species Roseburia hominis and Faecalibacterium prausnitzii defines dysbiosis in patients with ulcerative colitis.* Gut, 2014. **63**(8): p. 1275-83.
28. Trowell, H., *The development of the concept of dietary fiber in human nutrition.* The American Journal of Clinical Nutrition, 1978. **31**(10): p. S3-S11.
29. Cummings, J.H. and A. Engineer, *Denis Burkitt and the origins of the dietary fibre hypothesis.* Nutr Res Rev, 2018. **31**(1): p. 1-15.
30. Mason, P., *Probiotics and prebiotics.* The Pharmaceutical Journal, 2001. **266**(7132): p. 118--121.
31. Gibson, G.R., et al., *Dietary modulation of the human colonic microbiota: updating the concept of prebiotics.* Nutr Res Rev, 2004. **17**(2): p. 259-75.
32. Sarkar, A., et al., *Psychobiotics and the Manipulation of Bacteria-Gut-Brain Signals.* Trends Neurosci, 2016. **39**(11): p. 763-781.
33. Cryan, J.F. and S.M. O'Mahony, *The microbiome-gut-brain axis: from bowel to behavior.* Neurogastroenterol Motil, 2011. **23**(3): p. 187-92.
34. Foster, J.A. and K.A. McVey Neufeld, *Gut-brain axis: how the microbiome influences anxiety and depression.* Trends Neurosci, 2013. **36**(5): p. 305-12.
35. Jiang, H., et al., *Altered fecal microbiota composition in patients with major depressive disorder.* Brain Behav Immun, 2015. **48**: p. 186-94.
36. Bilder, D.A., et al., *Neuropsychiatric comorbidities in adults with phenylketonuria: A retrospective cohort study.* Mol Genet Metab, 2017. **121**(1): p. 1-8.
37. Clacy, A., R. Sharman, and J. McGill, *Depression, anxiety, and stress in young adults with phenylketonuria: associations with biochemistry.* J Dev Behav Pediatr, 2014. **35**(6): p. 388-91.
38. Lozupone, C.A., et al., *Diversity, stability and resilience of the human gut microbiota.* Nature, 2012. **489**(7415): p. 220-30.
39. Human Microbiome Project, C., *Structure, function and diversity of the healthy human microbiome.* Nature, 2012. **486**(7402): p. 207-14.
40. Sonnenburg, E.D. and J.L. Sonnenburg, *Starving our microbial self: the deleterious consequences of a diet deficient in microbiota-accessible carbohydrates.* Cell Metab, 2014. **20**(5): p. 779-86.
41. Miquel, S., et al., *Faecalibacterium prausnitzii and human intestinal health.* Curr Opin Microbiol, 2013. **16**(3): p. 255-61.
42. Pace, N.R., *A molecular view of microbial diversity and the biosphere.* Science, 1997. **276**(5313): p. 734-40.
43. Caporaso, J.G., et al., *Global patterns of 16S rRNA diversity at a depth of millions of sequences per sample.* Proc Natl Acad Sci U S A, 2011. **108 Suppl 1**: p. 4516-22.
44. Anderson, M.J., *Permutational Multivariate Analysis of Variance (PERMANOVA)*, in *Wiley StatsRef: Statistics Reference Online*. 2017. p. 1-15.
45. Love, M.I., W. Huber, and S. Anders, *Moderated estimation of fold change and dispersion for RNA-seq data with DESeq2.* Genome Biol, 2014. **15**(12): p. 550.
46. Washburne, A.D., et al., *Phylogenetic factorization of compositional data yields lineage-level associations in microbiome datasets.* PeerJ, 2017. **5**: p. e2969.
47. Douglas, G.M., et al., *PICRUSt2 for prediction of metagenome functions.* Nature Biotechnology, 2020. **38**(6): p. 685-688.
48. Bassanini, G., et al., *Phenylketonuria Diet Promotes Shifts in Firmicutes Populations.* Front Cell Infect Microbiol, 2019. **9**: p. 101.
49. Pinheiro de Oliveira, F., et al., *Phenylketonuria and Gut Microbiota: A Controlled Study Based on Next-Generation Sequencing.* PLoS One, 2016. **11**(6): p. e0157513.
50. Durrer, K.E., M.S. Allen, and I. Hunt von Herbing, *Genetically engineered probiotic for the treatment of phenylketonuria (PKU); assessment of a novel treatment in vitro and in the PAHenu2 mouse model of PKU.* PLoS One, 2017. **12**(5): p. e0176286.

51. Isabella, V.M., et al., *Development of a synthetic live bacterial therapeutic for the human metabolic disease phenylketonuria.* Nat Biotechnol, 2018. **36**(9): p. 857-864.
52. Statovci, D., et al., *The Impact of Western Diet and Nutrients on the Microbiota and Immune Response at Mucosal Interfaces.* Front Immunol, 2017. **8**: p. 838.
53. Lopez-Siles, M., et al., *Faecalibacterium prausnitzii: from microbiology to diagnostics and prognostics.* ISME J, 2017. **11**(4): p. 841-852.
54. Louis, P. and H.J. Flint, *Diversity, metabolism and microbial ecology of butyrate-producing bacteria from the human large intestine.* FEMS Microbiol Lett, 2009. **294**(1): p. 1-8.
55. Li, H.L., et al., *Alteration of Gut Microbiota and Inflammatory Cytokine/Chemokine Profiles in 5-Fluorouracil Induced Intestinal Mucositis.* Front Cell Infect Microbiol, 2017. **7**: p. 455.
56. Peng, L., et al., *Butyrate enhances the intestinal barrier by facilitating tight junction assembly via activation of AMP-activated protein kinase in Caco-2 cell monolayers.* J Nutr, 2009. **139**(9): p. 1619-25.
57. Valenzano, M.C., et al., *Remodeling of Tight Junctions and Enhancement of Barrier Integrity of the CACO-2 Intestinal Epithelial Cell Layer by Micronutrients.* PLoS One, 2015. **10**(7): p. e0133926.
58. Braniste, V., et al., *The gut microbiota influences blood-brain barrier permeability in mice.* Sci Transl Med, 2014. **6**(263): p. 263ra158.
59. Sullivan, J.E. and P. Chang, *Review: emotional and behavioral functioning in phenylketonuria.* J Pediatr Psychol, 1999. **24**(3): p. 281-99.
60. Kure, S., et al., *Tetrahydrobiopterin-responsive phenylalanine hydroxylase deficiency.* J Pediatr, 1999. **135**(3): p. 375-8.
61. Therrell, B.L., et al., *Current status of newborn screening worldwide: 2015.* Semin Perinatol, 2015. **39**(3): p. 171-87.
62. Hanley, W.B., *Adult phenylketonuria.* The American Journal of Medicine, 2004. **117**(8): p. 590-595.
63. Hanley, W.B., et al., *Vitamin B12 deficiency in adolescents and young adults with phenylketonuria.* Eur J Pediatr, 1996. **155 Suppl 1**: p. S145-7.
64. Acosta, P.B., et al., *Iron status of children with phenylketonuria undergoing nutrition therapy assessed by transferrin receptors.* Genet Med, 2004. **6**(2): p. 96-101.
65. Schindeler, S., et al., *The effects of large neutral amino acid supplements in PKU: an MRS and neuropsychological study.* Mol Genet Metab, 2007. **91**(1): p. 48-54.
66. Belanger, A.M., et al., *Inhibiting neutral amino acid transport for the treatment of phenylketonuria.* JCI Insight, 2018. **3**(14).
67. Longo, N., et al., *Single-dose, subcutaneous recombinant phenylalanine ammonia lyase conjugated with polyethylene glycol in adult patients with phenylketonuria: an open-label, multicentre, phase 1 dose-escalation trial.* The Lancet, 2014. **384**(9937): p. 37-44.
68. Sarkissian, C.N., et al., *A different approach to treatment of phenylketonuria: phenylalanine degradation with recombinant phenylalanine ammonia lyase.* Proc Natl Acad Sci U S A, 1999. **96**(5): p. 2339-44.
69. Qin, J., et al., *A metagenome-wide association study of gut microbiota in type 2 diabetes.* Nature, 2012. **490**(7418): p. 55-60.
70. Manichanh, C., et al., *The gut microbiota in IBD.* Nat Rev Gastroenterol Hepatol, 2012. **9**(10): p. 599-608.
71. Russell, S.L., et al., *Early life antibiotic-driven changes in microbiota enhance susceptibility to allergic asthma.* EMBO reports, 2012. **13**(5): p. 440-447.
72. Xu, M., et al., *Association Between Gut Microbiota and Autism Spectrum Disorder: A Systematic Review and Meta-Analysis.* Frontiers in psychiatry, 2019. **10**: p. 473-473.
73. Dickerson, F., E. Severance, and R. Yolken, *The microbiome, immunity, and schizophrenia and bipolar disorder.* Brain Behav Immun, 2017. **62**: p. 46-52.
74. Bercik, P., et al., *Chronic gastrointestinal inflammation induces anxiety-like behavior and alters central nervous system biochemistry in mice.* Gastroenterology, 2010. **139**(6): p. 2102-2112 e1.
75. Hemarajata, P. and J. Versalovic, *Effects of probiotics on gut microbiota: mechanisms of intestinal immunomodulation and neuromodulation.* Therap Adv Gastroenterol, 2013. **6**(1): p. 39-51.
76. Martin, M., *Cutadapt removes adapter sequences from high-throughput sequencing reads.* EMBnet.journal, 2011. **17**(1): p. 10-12.
77. Callahan, B.J., et al., *DADA2: High-resolution sample inference from Illumina amplicon data.* Nat Methods, 2016. **13**(7): p. 581-3.

78. R Core Team, *R: A language and environment for statistical computing*. 2018, R Foundation for Statistical Computing: Vienna, Austria.
79. Rognes, T., et al., *VSEARCH: a versatile open source tool for metagenomics.* PeerJ, 2016. **4**: p. e2584.
80. McMurdie, P.J. and S. Holmes, *phyloseq: an R package for reproducible interactive analysis and graphics of microbiome census data.* PLoS One, 2013. **8**(4): p. e61217.
81. Silverman, J.D., et al., *A phylogenetic transform enhances analysis of compositional microbiota data.* Elife, 2017. **6**.
82. OksanenJ, B.F., Friendly M, Kindt R, Legendre P, McGlinnD, et al, *vegan: Community Ecology Package*. 2019.
83. Parks, D.H. and R.G. Beiko, *Identifying biologically relevant differences between metagenomic communities.* Bioinformatics, 2010. **26**(6): p. 715-21.
84. Haas, K.N. and J.L. Blanchard, *Reclassification of the Clostridium clostridioforme and Clostridium sphenoides clades as Enterocloster gen. nov. and Lacrimispora gen. nov., including reclassification of 15 taxa.* Int J Syst Evol Microbiol, 2020. **70**(1): p. 23-34.
85. Pryde, S.E., et al., *The microbiology of butyrate formation in the human colon.* FEMS Microbiol Lett, 2002. **217**(2): p. 133-9.
86. McIntyre, A., P.R. Gibson, and G.P. Young, *Butyrate production from dietary fibre and protection against large bowel cancer in a rat model.* Gut, 1993. **34**(3): p. 386-91.
87. Matt, S.M., et al., *Butyrate and Dietary Soluble Fiber Improve Neuroinflammation Associated With Aging in Mice.* Front Immunol, 2018. **9**: p. 1832.
88. Breyner, N.M., et al., *Microbial Anti-Inflammatory Molecule (MAM) from Faecalibacterium prausnitzii Shows a Protective Effect on DNBS and DSS-Induced Colitis Model in Mice through Inhibition of NF-kappaB Pathway.* Front Microbiol, 2017. **8**: p. 114.
89. Fujimoto, T., et al., *Decreased abundance of Faecalibacterium prausnitzii in the gut microbiota of Crohn's disease.* J Gastroenterol Hepatol, 2013. **28**(4): p. 613-9.
90. Sokol, H., et al., *Low counts of Faecalibacterium prausnitzii in colitis microbiota.* Inflamm Bowel Dis, 2009. **15**(8): p. 1183-9.
91. Schirmer, M., et al., *Dynamics of metatranscription in the inflammatory bowel disease gut microbiome.* Nat Microbiol, 2018. **3**(3): p. 337-346.
92. Gerritsen, J., et al., *Romboutsia hominis sp. nov., the first human gut-derived representative of the genus Romboutsia, isolated from ileostoma effluent.* Int J Syst Evol Microbiol, 2018. **68**(11): p. 3479-3486.
93. Gerritsen, J., et al., *A comparative and functional genomics analysis of the genus Romboutsia provides insight into adaptation to an intestinal lifestyle.* 2019.
94. Vacca, M., et al., *The Controversial Role of Human Gut Lachnospiraceae.* Microorganisms, 2020. **8**(4).
95. Yatsunenko, T., et al., *Human gut microbiome viewed across age and geography.* Nature, 2012. **486**(7402): p. 222-7.
96. Burton, B.K., et al., *Prevalence of comorbid conditions among adult patients diagnosed with phenylketonuria.* Mol Genet Metab, 2018. **125**(3): p. 228-234.
97. Kau, A.L., et al., *Human nutrition, the gut microbiome and the immune system.* Nature, 2011. **474**(7351): p. 327-36.
98. Oleskin, A.V. and B.A. Shenderov, *Probiotics and Psychobiotics: the Role of Microbial Neurochemicals.* Probiotics Antimicrob Proteins, 2019. **11**(4): p. 1071-1085.
99. Byers, H.L., et al., *N-acetylneuraminic acid transport by Streptococcus oralis strain AR3.* J Med Microbiol, 1999. **48**(4): p. 375-381.
100. Trefz, K.F., et al., *Clinical burden of illness in patients with phenylketonuria (PKU) and associated comorbidities - a retrospective study of German health insurance claims data.* Orphanet J Rare Dis, 2019. **14**(1): p. 181.
101. Candela, M., et al., *Interaction of probiotic Lactobacillus and Bifidobacterium strains with human intestinal epithelial cells: adhesion properties, competition against enteropathogens and modulation of IL-8 production.* Int J Food Microbiol, 2008. **125**(3): p. 286-92.
102. Fukuda, S., et al., *Bifidobacteria can protect from enteropathogenic infection through production of acetate.* Nature, 2011. **469**(7331): p. 543-7.
103. Sonnenburg, J.L., et al., *Glycan foraging in vivo by an intestine-adapted bacterial symbiont.* Science, 2005. **307**(5717): p. 1955-9.
104. Olszak, T., et al., *Microbial exposure during early life has persistent effects on natural killer T cell function.* Science, 2012. **336**(6080): p. 489-93.

105. Silva, Y.P., A. Bernardi, and R.L. Frozza, *The Role of Short-Chain Fatty Acids From Gut Microbiota in Gut-Brain Communication.* Front Endocrinol (Lausanne), 2020. **11**: p. 25.
106. Opazo, M.C., et al., *Intestinal Microbiota Influences Non-intestinal Related Autoimmune Diseases.* Front Microbiol, 2018. **9**: p. 432.
107. Arpaia, N., et al., *Metabolites produced by commensal bacteria promote peripheral regulatory T-cell generation.* Nature, 2013. **504**(7480): p. 451-5.
108. Bercik, P., S.M. Collins, and E.F. Verdu, *Microbes and the gut-brain axis.* Neurogastroenterol Motil, 2012. **24**(5): p. 405-13.
109. Neufeld, K.A., et al., *Effects of intestinal microbiota on anxiety-like behavior.* Commun Integr Biol, 2011. **4**(4): p. 492-4.
110. Gill, S.R., et al., *Metagenomic analysis of the human distal gut microbiome.* Science, 2006. **312**(5778): p. 1355-9.
111. Muegge, B.D., et al., *Diet drives convergence in gut microbiome functions across mammalian phylogeny and within humans.* Science, 2011. **332**(6032): p. 970-4.
112. David, L.A., et al., *Diet rapidly and reproducibly alters the human gut microbiome.* Nature, 2014. **505**(7484): p. 559-63.
113. Wu, G.D., et al., *Linking long-term dietary patterns with gut microbial enterotypes.* Science, 2011. **334**(6052): p. 105-8.
114. Desai, M.S., et al., *A Dietary Fiber-Deprived Gut Microbiota Degrades the Colonic Mucus Barrier and Enhances Pathogen Susceptibility.* Cell, 2016. **167**(5): p. 1339-1353 e21.
115. Cotillard, A., et al., *Dietary intervention impact on gut microbial gene richness.* Nature, 2013. **500**(7464): p. 585-8.
116. Litvak, Y., M.X. Byndloss, and A.J. Baumler, *Colonocyte metabolism shapes the gut microbiota.* Science, 2018. **362**(6418).
117. Trompette, A., et al., *Gut microbiota metabolism of dietary fiber influences allergic airway disease and hematopoiesis.* Nat Med, 2014. **20**(2): p. 159-66.
118. Luhrs, H., et al., *Butyrate inhibits NF-kappaB activation in lamina propria macrophages of patients with ulcerative colitis.* Scand J Gastroenterol, 2002. **37**(4): p. 458-66.
119. Eeckhaut, V., et al., *Butyricicoccus pullicaecorum in inflammatory bowel disease.* Gut, 2013. **62**(12): p. 1745-52.
120. Verduci, E., et al., *Phenylketonuric diet negatively impacts on butyrate production.* Nutr Metab Cardiovasc Dis, 2018. **28**(4): p. 385-392.
121. Benus, R.F., et al., *Association between Faecalibacterium prausnitzii and dietary fibre in colonic fermentation in healthy human subjects.* Br J Nutr, 2010. **104**(5): p. 693-700.
122. Zhao, G., M. Nyman, and J.A. Jonsson, *Rapid determination of short-chain fatty acids in colonic contents and faeces of humans and rats by acidified water-extraction and direct-injection gas chromatography.* Biomed Chromatogr, 2006. **20**(8): p. 674-82.
123. Han, F., et al., *Porcine beta-defensin 2 attenuates inflammation and mucosal lesions in dextran sodium sulfate-induced colitis.* J Immunol, 2015. **194**(4): p. 1882-93.
124. Biton, I.E., et al., *Assessing Mucosal Inflammation in a DSS-Induced Colitis Mouse Model by MR Colonography.* Tomography, 2018. **4**(1): p. 4-13.
125. Mancilla, V.J., et al., *The Adult Phenylketonuria (PKU) Gut Microbiome.* Microorganisms, 2021. **9**(3).
126. Colonetti, K., L.F. Roesch, and I.V.D. Schwartz, *The microbiome and inborn errors of metabolism: Why we should look carefully at their interplay?* Genet Mol Biol, 2018. **41**(3): p. 515-532.
127. Moya, A. and M. Ferrer, *Functional Redundancy-Induced Stability of Gut Microbiota Subjected to Disturbance.* Trends Microbiol, 2016. **24**(5): p. 402-413.
128. Iljazovic, A., et al., *Perturbation of the gut microbiome by Prevotella spp. enhances host susceptibility to mucosal inflammation.* Mucosal Immunol, 2021. **14**(1): p. 113-124.
129. Kim, Y., et al., *Dietary cellulose prevents gut inflammation by modulating lipid metabolism and gut microbiota.* Gut Microbes, 2020. **11**(4): p. 944-961.
130. Slavin, J., *Fiber and prebiotics: mechanisms and health benefits.* Nutrients, 2013. **5**(4): p. 1417-35.
131. Takiishi, T., C.I.M. Fenero, and N.O.S. Camara, *Intestinal barrier and gut microbiota: Shaping our immune responses throughout life.* Tissue Barriers, 2017. **5**(4): p. e1373208.
132. Zhao, L., et al., *Gut bacteria selectively promoted by dietary fibers alleviate type 2 diabetes.* Science, 2018. **359**(6380): p. 1151-1156.
133. Bourin, M., et al., *Animal models of anxiety in mice.* Fundam Clin Pharmacol, 2007. **21**(6): p. 567-74.

134. Stewart, C.J., et al., *Temporal development of the gut microbiome in early childhood from the TEDDY study.* Nature, 2018. **562**(7728): p. 583-588.
135. Christ, S.E., et al., *The effects of tetrahydrobiopterin (BH4) treatment on brain function in individuals with phenylketonuria.* Neuroimage Clin, 2013. **3**: p. 539-47.
136. Brosco, J.P. and D.B. Paul, *The political history of PKU: reflections on 50 years of newborn screening.* Pediatrics, 2013. **132**(6): p. 987-9.
137. Tap, J., et al., *Towards the human intestinal microbiota phylogenetic core.* Environ Microbiol, 2009. **11**(10): p. 2574-84.
138. Walker, A.W., et al., *Dominant and diet-responsive groups of bacteria within the human colonic microbiota.* ISME J, 2011. **5**(2): p. 220-30.
139. Duncan, S.H., *Growth requirements and fermentation products of Fusobacterium prausnitzii, and a proposal to reclassify it as Faecalibacterium prausnitzii gen. nov., comb. nov.* International Journal of Systematic and Evolutionary Microbiology, 2002. **52**(6): p. 2141-2146.
140. Quevrain, E., et al., *Identification of an anti-inflammatory protein from Faecalibacterium prausnitzii, a commensal bacterium deficient in Crohn's disease.* Gut, 2016. **65**(3): p. 415-425.
141. Sokol, H., et al., *Faecalibacterium prausnitzii is an anti-inflammatory commensal bacterium identified by gut microbiota analysis of Crohn disease patients.* Proceedings of the National Academy of Sciences of the United States of America, 2008. **105**(43): p. 16731-16736.
142. Bojovic, K., et al., *Gut Microbiota Dysbiosis Associated With Altered Production of Short Chain Fatty Acids in Children With Neurodevelopmental Disorders.* Front Cell Infect Microbiol, 2020. **10**: p. 223.